ANCR-1207

ANCR-1207
NRC-4

TRANSIENT THREE-DIMENSIONAL THERMAL-HYDRAULIC ANALYSIS OF NUCLEAR REACTOR FUEL ROD ARRAYS: GENERAL EQUATIONS AND NUMERICAL SCHEME

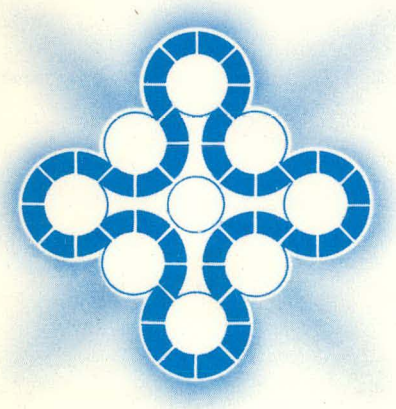

Aerojet Nuclear Company

IDAHO NATIONAL ENGINEERING LABORATORY

Idaho Falls, Idaho — 83401

DATE PUBLISHED—NOVEMBER 1975

PREPARED FOR THE
ENERGY RESEARCH AND DEVELOPMENT ADMINISTRATION
IDAHO OPERATIONS OFFICE UNDER CONTRACT E (10-1)-1375

DISCLAIMER

Printed in the United States of America
Available from
National Technical Information Service
U. S. Department of Commerce
5285 Port Royal Road
Springfield, Virginia 22161
Price: Printed Copy $5.45; Microfiche $2.25

ANCR-1207

Distributed Under Category:
NRC-4
Water Reactor Safety Research
Analysis Development
TID-4500, R63

TRANSIENT THREE-DIMENSIONAL THERMAL-HYDRAULIC ANALYSIS OF NUCLEAR REACTOR FUEL ROD ARRAYS: GENERAL EQUATIONS AND NUMERICAL SCHEME

by

Walter J. Wnek
John D. Ramshaw
John A. Trapp
E. Daniel Hughes
Charles W. Solbrig

AEROJET NUCLEAR COMPANY

Date Published - November 1975

PREPARED FOR THE
U.S. ENERGY RESEARCH AND DEVELOPMENT ADMINISTRATION
IDAHO OPERATIONS OFFICE
UNDER CONTRACT NO. E(10-1)-1375

ABSTRACT

A mathematical model and a numerical solution scheme for thermal-hydraulic analysis of fuel rod arrays are given. The model alleviates the two major deficiencies associated with existing rod array analysis models, that of a correct transverse momentum equation and the capability of handling reversing and circulatory flows. Possible applications of the model include steady state and transient subchannel calculations as well as analysis of flows in heat exchangers, other engineering equipment, and porous media.

NOMENCLATURE

A_h	=	heated surface area per unit volume
A_w	=	wetted surface area per unit volume
B_w^{ij}	=	friction drag factor
C_p	=	specific heat
C_I	=	speed of sound at constant specific internal energy
D	=	divergence of v
d_{ij}	=	$\frac{1}{2}(v_{i,j} + v_{j,i})$
F_i	=	drag force in the i^{th} direction
f_w^i	=	friction factor in i^{th} direction
g_i	=	body force in the i^{th} direction
h	=	heat transfer coefficient for solid-fluid interface
I	=	specific internal energy
I_B	=	specified boundary specific internal energy
k	=	molecular thermal conductivity
k_t	=	turbulent or eddy thermal diffusivity
M_i	=	fluctuating terms in momentum equation
n_i	=	components of outward unit normal
p	=	pressure
p_B	=	specified boundary pressure
Pr	=	Prandtl number, $\frac{\mu C_p}{k}$
$\underset{\sim}{q}$	=	local heat flux vector with coordinates q_i

Q_g	=	volumetric energy supply
Q_w	=	rate of wall heat supply per unit volume
Re_w	=	Reynolds number
S_f	=	fluid surface enclosing V_f
S_{ff}	=	part of S_f occupied by fluid only
S_{sf}	=	solid-fluid interface
t	=	time
T_b	=	coolant bulk temperature
T_S	=	solid surface temperature
u_B	=	specified boundary velocity
V	=	control volume used in averaging procedure
V_f	=	volume of fluid in V
$\underset{\sim}{v}$	=	fluid velocity vector with coordinates v_i or u, v, w
$\underset{\sim}{V}^s$	=	solid-fluid interface velocity vector with coordinates V_i^s
x	=	thermodynamic quality
$\underset{\sim}{x}$	=	position vector with coordinates x_i
$\underset{\sim}{y}$	=	a position vector to the center of V with coordinates y_i

Greek Letters

$\Delta\tau$	=	weighting factor in iteration scheme
Δt	=	time increment
Δx_i	=	space increment in x_i direction
ϵ	=	porosity = V_f/V
μ	=	molecular viscosity
μ_t	=	turbulent or eddy viscosity
ν (or ν_t)	=	kinematic viscosity = μ/ρ or (or μ_t/ρ)
ξ	=	iteration weighting factor or relative roughness coefficient
ρ	=	density
ρ_B	=	specified boundary density
σ_{ij}	=	stress tensor
σ_y^T	=	turbulent stress tensor
$\phi_{\ell o}^2$	=	two-phase friction multiplier

Other Symbols

$\overline{\quad}$	=	denotes an average taken over V; that is, mixture average
$\tilde{\quad}$	=	denotes an average taken over V_f; that is, fluid average
$'$	=	denotes a fluctuating part
$\hat{\quad}$	=	denotes the most recent iteration
$\equiv$	=	definition

CONTENTS

FIGURES

TRANSIENT THREE-DIMENSIONAL THERMAL-HYDRAULIC ANALYSIS OF NUCLEAR REACTOR FUEL ROD ARRAYS: GENERAL EQUATIONS AND NUMERICAL SCHEME

I. INTRODUCTION

Recent advances in numerical solution techniques for systems of quasi-linear partial differential equations have led to more refined analyses of complex engineering problems. Currently available computers and numerical solution techniques have made construction of mathematical models more nearly exact so that less empiricism is required, and the empirical relations that are needed are of a more basic nature. Thus, the resulting computer programs can be used for extrapolative engineering design studies with increased confidence. The area of turbulent flow analysis is a good example of the application of such models to complex problems[1].

The nuclear industry employs a large number of computer codes for both steady state design work and transient-incident safety analysis. A variety of codes have been written in order to analyze complete nuclear steam supply systems or selected subsystems such as the primary pressure vessel, emergency core cooling system, and the reactor core. The thermal-hydraulic characteristics of the core are important with respect to both steady state design operation and transient response to an incident. In the former case, core thermal-hydraulic considerations dictate, to a large extent, the possible steady operating power obtainable from a given core design. In the case of incidents, thermal-hydraulic considerations are important because the core contains fission products that must not be allowed to escape into the atmosphere. Because the thermal-hydraulic characteristics of the core are so important, many experimental and analytical studies have been conducted on the parallel-rod-array geometry that is typical of a large number of reactor core designs. Thermal-hydraulic analysis and experimental studies of rod arrays are difficult to perform due to the geometric complexity of the rod array and the two-phase nature of the coolant employed in many nuclear reactors.

The geometric complexity arises from the large number of degrees of freedom associated with parallel-rod arrays. Among the geometric variables that are known to affect the thermal-hydraulic characteristics of rod arrays are the rod diameter, rod-to-rod pitch, spacing between rods, rod spacer type and location, and, for arrays within shrouds, the spacing between rods and shroud, and the shroud geometry. The rod power generation varies radially and axially throughout the array thereby causing the coolant flow rate and thermodynamic state to vary throughout the array.

Two-phase flow of the coolant compounds the analytical and experimental difficulties due to the introduction of additional thermal-hydraulic variables, such as the vapor volume fraction, velocity and temperature differences between the phases, and distribution of the phases within the flow field. A vast amount of data and associated literature exists on two-phase flow, and empirical correlations have been developed for friction factors, void

fractions, liquid-vapor velocity slip, heat transfer coefficients, mass and energy mixing, critical heat flux, and flow regime.

Because of the overall complexity of rod array analysis, many computer programs have been developed for steady state design studies and transient incident analysis. Representative of the codes in use are COBRA[2], COBRA-II[3], COBRA III[4,5], HAMBO[6,7], MICRO-3[8], LEUCIPPO[9], TEMP[10], and HOTROD[11]. All of these codes are based on a fluid flow model that assumes that the rod array can be represented by parallel interconnected channels. The Navier-Stokes equations are simplified to be consistent with this assumption and the resulting equation system is, in general, solved as an initial value problem with distance from the rod array inlet as the independent coordinate. Bowring[12] and Berger[13] have noted that this procedure can introduce errors if downstream effects such as spacers and flow blockages are not given careful consideration. The simplifications in the Navier-Stokes equations introduced by this assumption usually result in an incomplete representation of the momentum component in the transverse or radial direction and an inability to handle flow reversals. "Transverse" refers to the direction normal to the primary direction of flow under steady state conditions. However, during some transients, conditions in the core may result in a very low velocity and possibly natural convection, so that the distinction between transverse and primary becomes less clear.

The method of analysis presented in this report differs from those used in the existing codes previously discussed in that the governing equations are obtained by volume averaging the complete fluid-mechanical equations of continuity, momentum, and energy. The resulting averaged equations are three-dimensional. The equations are applied without invoking assumptions that would reduce the model to the parallel channel case. The equations are solved as an initial value problem in time and a boundary value problem in space. As a result, transport in the radial or transverse direction, due to turbulence and radial pressure gradients, is taken into account more rigorously than in previous treatments, and flow reversals in the core are easily handled.

The mathematical description is quite general in that transient flow of a compressible fluid is assumed, and the distributions of the solids embedded in the flow and the heat energy sources can be any functions of position and time. In addition, to use for calculation of flows in nuclear reactor cores as discussed in the report, a wide variety of other applications of the model is possible. Among these are calculation of flows in porous media, heat exchangers, and other engineering equipment, and calculation of local phenomena in flows amenable to a Prandtl mixing length turbulence description.

The report is organized into the following sections. Section II gives the development of the volume-averaged Navier-Stokes equations; Section III discusses the constitutive equations required to close the equation system; and Section IV presents the numerical solution scheme. Example applications are given in Section V.

II. BASIC EQUATIONS

The differential equations described in this section are derived by considering a control volume V whose dimensions are small compared to the large scale phenomena of interest and large relative to the local phenomena, which are not of interest. The notion of large or small is relative. If a core-wide PWR analysis is of interest, then the control volume V might be composed of an axial section of several fuel assemblies, and phenomena on the scale of the rod channels within a bundle would be represented by average quantities. If a BWR single bundle or subchannel analysis is of interest, the typical control volume V would consist of an axial section of a single flow channel and parts of the adjacent rods. In this case, phenomena within a given flow channel would be represented by average quantities. In both these cases, the averaging process used on the equations is the same, but the correlations used to represent some of the averaged phenomena could be different. For this reason, the development of the averaged equations derived in this section is basically independent of the size of the control volume used in practice so long as appropriate correlations are employed in different applications.

Before the averaged equations are developed from local equations, some basic mathematical results concerning volume averages are needed. The development given here follows that presented by Slattery[14]. About each point y in the flow region (both solids and fluids occupy the flow region), a control volume, V, is constructed as shown in Figure 1. All control volumes V have the same shape and orientation. (In Figure 1, the volume has been shown to be spherical, but any fixed shape could be used in the averaging.) As shown in Figure 1, a typical volume will contain regions of fluid and also regions occupied by the solid. The region of V occupied by fluid is denoted by $V_f(\underset{\sim}{y},t)$, and the surface of this region is denoted by $S_f(\underset{\sim}{y},t)$. The surface $S_f(\underset{\sim}{y},t)$ is further specified as the sum of $S_{sf}(\underset{\sim}{y},t)$ which denotes that part of $S_f(\underset{\sim}{y},t)$ on the interface between the solid and fluid and $S_{ff}(\underset{\sim}{y},t)$ which denotes that part of $S_f(\underset{\sim}{y},t)$ occupied by the fluid.

The volume average of any scalar, vector, or tensor property $\Psi(\underset{\sim}{x},t)$ associated with the flow field is defined as

$$\overline{\Psi}(\underset{\sim}{y},t) \equiv \frac{1}{V}\int_{V_f(\underset{\sim}{y},t)} \Psi(\underset{\sim}{x},t)\, dV \quad . \tag{1}$$

The averaging process to be employed requires derivatives of the average property $\overline{\Psi}(\underset{\sim}{y},t)$ with respect to time, t, and position, y_i. General expressions for these derivatives are obtained as follows.

The time derivative, $\frac{\partial}{\partial t}\overline{\Psi}(\underset{\sim}{y},t)$, is calculated by use of the generalized Reynolds transport theorem in the form

$$\frac{\partial}{\partial t}\frac{1}{V}\int_{V_f(\underset{\sim}{y},t)} \Psi(\underset{\sim}{x},t)\, dV = \frac{1}{V}\int_{V_f(\underset{\sim}{y},t)} \frac{\partial}{\partial t}\Psi(\underset{\sim}{x},t)\, dV + \frac{1}{V}\int_{S_f(\underset{\sim}{y},t)} \Psi(\underset{\sim}{x},t)\, V^s_k n_k\, dS \tag{2}$$

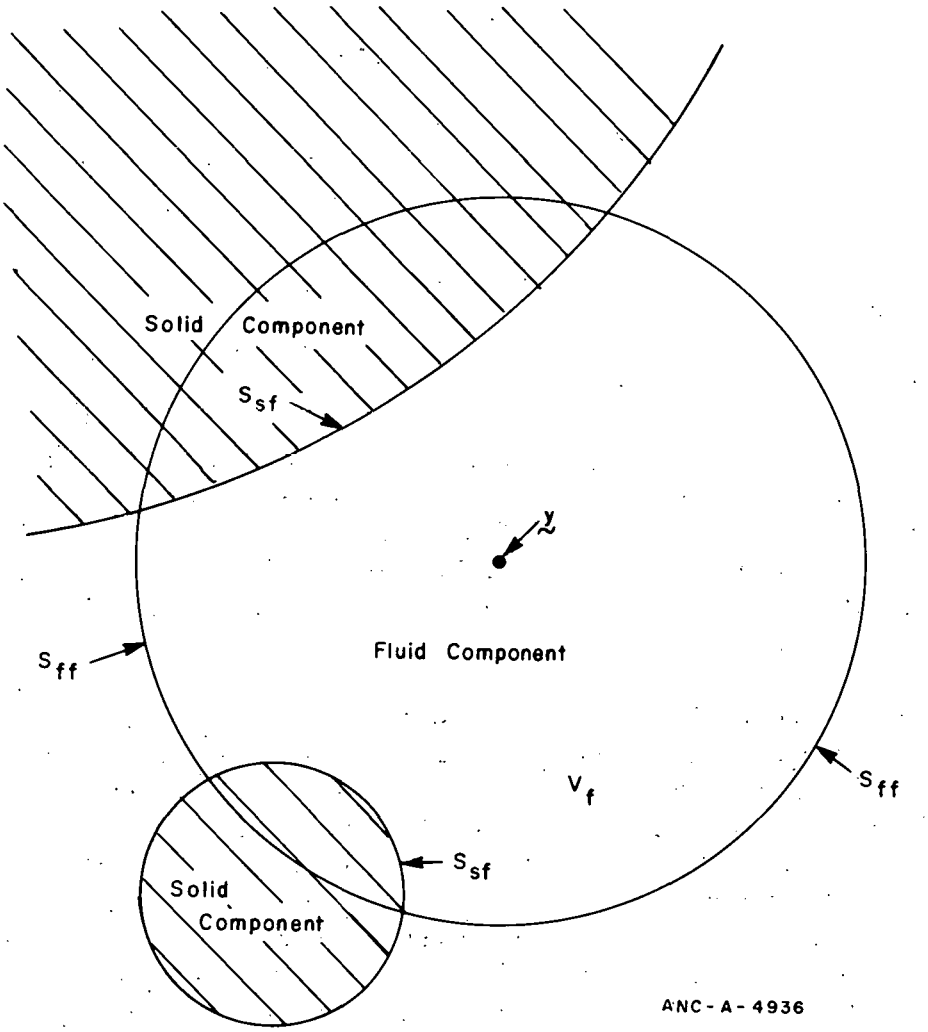

Fig. 1 Typical control volume.

where V_k^s is the velocity of the surface S_f, and n_k is the outward directed unit normal to S_f. The velocity V_k^s is zero on that part of S_f denoted by $S_{ff}(\underset{\sim}{y},t)$ and, in the absence of chemical reactions, on $S_{sf}(\underset{\sim}{y},t)$, V_k^s is equal to the fluid velocity v_k, which may be nonzero due to time rate of change of porosity, ϵ. With these values of V_k^s, Equation (2) becomes

$$\frac{\partial}{\partial t}\frac{1}{V}\int_{V_f(\underset{\sim}{y},t)}\Psi(\underset{\sim}{x},t)\,dV = \frac{1}{V}\int_{V_f(\underset{\sim}{y},t)}\frac{\partial}{\partial t}\Psi(\underset{\sim}{x},t)\,dV + \frac{1}{V}\int_{S_{sf}(\underset{\sim}{y},t)}\Psi(\underset{\sim}{x},t)\,v_k n_k dS. \tag{3}$$

An expression for the spatial derivative $\frac{\partial}{\partial y_i}\overline{\Psi}$ can be obtained as in Reference 14. The results are given by

$$\frac{\partial}{\partial y_k}\frac{1}{V}\int_{V_f(\underset{\sim}{y},t)}\Psi(\underset{\sim}{x},t)\,dV = \frac{1}{V}\int_{S_{ff}(\underset{\sim}{y},t)}\Psi(\underset{\sim}{x},t)\,n_k dS. \tag{4}$$

Adding $\frac{1}{V}\int_{S_{sf}} \Psi(\underset{\sim}{x},t)\, n_k dS$ to both sides of Equation (4) and applying the divergence theorem results in

$$\frac{\partial}{\partial y_k}\frac{1}{V}\int_{V_f(\underset{\sim}{y},t)} \Psi(\underset{\sim}{x},t)\ dV = \frac{1}{V}\int_{V_f(\underset{\sim}{y},t)} \frac{\partial}{\partial x_k}\Psi(\underset{\sim}{x},t)\ dV - \frac{1}{V}\int_{S_{sf}(\underset{\sim}{y},t)} \Psi(\underset{\sim}{x},t) n_k dS. \tag{5}$$

Equations (3) and (5) are the formulas needed in the volume averaging of the local equations to be carried out subsequently .These equations are quite general as no restrictive assumptions were employed in the derivation.

The results of the volume-averaging procedure are more convenient if expressed in terms of quantities that refer to fluid average properties instead of mixture average properties. The mixture average quantities in Equations (1) through (5) can be converted to fluid average values as follows. The fluid volume fraction, or porosity, is given by

$$\varepsilon \equiv \frac{V_f}{V} = \frac{1}{V}\int_{V_f(\underset{\sim}{y},t)} dV. \tag{6}$$

The fluid average value of a property Ψ is defined as

$$\bar{\Psi}(\underset{\sim}{y},t) \equiv \frac{1}{V_f}\int_{V_f(\underset{\sim}{y},t)} \Psi(\underset{\sim}{x},t)\ dV \tag{7}$$

so that Equations (1) and (7), when used with Equation (6), give

$$\bar{\Psi}(\underset{\sim}{y},t) = \varepsilon\, \tilde{\Psi}(\underset{\sim}{y},t). \tag{8}$$

Equation (8) is the relationship between the mixture average, $\bar{\Psi}$, and the fluid average, $\tilde{\Psi}$.

Formulas for the time and spatial derivatives of the porosity, $\frac{\partial \varepsilon}{\partial t}$ and $\frac{\partial \varepsilon_l}{\partial y_i}$, respectively, can also be obtained from Equation (6). The time derivative is obtained by application of Equation (3) with $\Psi(\underset{\sim}{x},t)=1$ as given by Equation (6). Simplification of the resulting equation gives

$$\frac{\partial \varepsilon}{\partial t} = \frac{1}{V}\int_{S_{sf}(\underset{\sim}{y},t)} v_k n_k dS. \tag{9}$$

Equation (9) explicitly shows the relationship between the time rate of change of the porosity and the motion of the solid-fluid interface that was discussed when Equation (3) was obtained. Application of Equation (5) yields the spatial derivative

$$\frac{\partial \varepsilon}{\partial y_k} = -\frac{1}{V}\int_{S_{sf}(y,t)} n_k dS \ . \tag{10}$$

The equations developed in this section are now applied to volume averaging of the local Navier-Stokes equations.

1. VOLUME-AVERAGED CONSERVATION OF MASS

The volume-averaged equation for conservation of mass will be developed in detail. The local equation that applies at all points, such as shown in Figure 1, is given by

$$\frac{\partial \rho}{\partial t} + \frac{\partial}{\partial x_k}(\rho v_k) = 0 \ . \tag{11}$$

The volume-averaged equation is obtained by integrating Equation (11) over V_f so that

$$\frac{1}{V}\int_{V_f(y,t)} \frac{\partial}{\partial t}\rho \, dV + \frac{1}{V}\int_{V_f(y,t)} \frac{\partial}{\partial x_k}(\rho v_k) dV = 0 \ . \tag{12}$$

Equation (12) is rearranged by using Equation (3) on the first integral and Equation (5) on the second integral to obtain

$$\frac{\partial}{\partial t}\frac{1}{V}\int_{V_f(y,t)} \rho dV + \frac{\partial}{\partial y_k}\frac{1}{V}\int_{V_f(y,t)} \rho v_k dV = 0 \ , \tag{13}$$

or, by using the definition

$$\frac{\partial}{\partial t}\overline{\rho} + \frac{\partial}{\partial y_k}\overline{\rho v_k} = 0 \ . \tag{14}$$

Equation (14) is the mixture-averaged conservation of mass equation. By using Equation (8), Equation (14) can be expressed in terms of fluid averages as

$$\frac{\partial}{\partial t}(\varepsilon\tilde{\rho}) + \frac{\partial}{\partial y_k}(\varepsilon \widetilde{\rho v_k}) = 0 \ . \tag{15}$$

Equation (15) contains the spatial average of the product of density and velocity. The momentum equation, likewise, will contain spatial averages of the product of density and two velocity components. The net result is that the averaging process introduces more

unknowns than available equations. This problem can be partially solved by expressing the instantaneous dependent variables as the sum of an average contribution plus a fluctuating part. That is, when

$$\rho = \tilde{\rho} + \rho' \quad ; \quad (\widetilde{\rho'} = 0), \tag{16a}$$

and

$$v_k = \tilde{v}_k + v_k' \quad ; \quad (\widetilde{v_k'} = 0), \tag{16b}$$

where the primed quantities are the difference in V_f between the actual value and the fluid average value, then Equation (15) becomes

$$\frac{\partial}{\partial t} (\varepsilon \tilde{\rho}) + \frac{\partial}{\partial y_k} (\varepsilon \tilde{\rho} \tilde{v}_k) = - \frac{\partial}{\partial y_k} (\varepsilon \widetilde{\rho' v_k'}) . \tag{17}$$

The term on the right-hand side of Equation (17) is analogous to corresponding terms in compressible turbulent flow and porous media equations. In turbulent flow, the term is usually obtained from time averaging of the Navier-Stokes equations. Here, it is the result of nonuniform spatial distributions of v_k and ρ as the fluid moves through the void space between the solids. This term is nonzero even if the local flow is laminar. In the following analysis, this term is considered small compared to other terms in the equation and is neglected. The resulting mass conservation equation in terms of fluid average properties becomes

$$\frac{\partial}{\partial t} (\varepsilon \tilde{\rho}) + \frac{\partial}{\partial y_k} (\varepsilon \tilde{\rho} \tilde{v}_k) = 0 . \tag{18}$$

Equation (18) is the desired result for the conservation of mass equation. Comparison of predictions from Equation (18) with experimental data, such as rod array subchannel data, may indicate that a model of the term on the right-hand side of Equation (17) is necessary.

2. VOLUME-AVERAGED LINEAR MOMENTUM BALANCE

The fluid average linear momentum equations will be developed from the local continuum equations. The process is similar to that used to obtain the conservation of mass equation and is not given in as much detail.

The local momentum equations are given by

$$\frac{\partial}{\partial t} (\rho v_i) + \frac{\partial}{\partial x_k} (\rho v_i) v_k = - \frac{\partial p}{\partial x_i} + \frac{\partial \sigma_{ki}}{\partial x_k} + \rho g_i . \tag{19}$$

Integrating Equation (19) over V_f and applying Equations (3) and (5) to the time and space derivatives, respectively, results in

$$\frac{\partial}{\partial t}\overline{\rho\, v_i} + \frac{\partial}{\partial y_k}\overline{\rho\, v_i v_k} = -\frac{\partial}{\partial y_i}\overline{p} + \frac{\partial}{\partial y_k}\overline{\sigma_{ik}} + \overline{\rho}\, g_i \qquad (20)$$

$$+ \frac{1}{V}\int_{S_{sf}} [-\, p\, n_i + \sigma_{ik} n_k]\, dS \ .$$

When the integral term in Equation (20) is denoted by I_i and when Equation (8) is used to introduce fluid averages, Equation (20) can be rewritten as

$$\frac{\partial \widetilde{\varepsilon\rho\, v_i}}{\partial t} + \frac{\partial \widetilde{\varepsilon\rho\, v_i v_k}}{\partial y_k} = -\frac{\partial \tilde{\varepsilon}\tilde{p}}{\partial y_i} + \frac{\partial \tilde{\varepsilon}\,\tilde{\sigma}_{ik}}{\partial y_k} + \tilde{\varepsilon}\,\tilde{\rho}\, g_i + I_i \qquad (21)$$

or, by the use of Equation (16) as

$$\frac{\partial \tilde{\varepsilon}\tilde{\rho}\,\tilde{v}_i}{\partial t} + \frac{\partial \tilde{\varepsilon}\tilde{\rho}\,\tilde{v}_i\tilde{v}_k}{\partial y_k} = -\frac{\partial \tilde{\varepsilon}\tilde{p}}{\partial y_i} + \frac{\partial \tilde{\varepsilon}\,\tilde{\sigma}_{ik}}{\partial y_k} + \tilde{\varepsilon}\tilde{\rho}\, g_i + I_i \qquad (22)$$

$$- \frac{\partial}{\partial t}\left(\widetilde{\varepsilon\rho'\, v_i'}\right) - \frac{\partial}{\partial y_k}\left[\left(\widetilde{\varepsilon\rho\, v_i' v_k'}\right) + \left(\widetilde{\varepsilon v_i\, \rho' v_k'}\right) + \left(\widetilde{\varepsilon v_k\, \rho' v_i'}\right) + \widetilde{\varepsilon\rho' v_i' v_k'}\right]$$

The term I_i in Equation (22) represents the solid-fluid interfacial momentum exchange per unit volume and may be simplified as follows. The pressure, p, is written as the sum of a spatial average plus a fluctuating part:

$$p = \tilde{p} + p' \ ; \ (\widetilde{p'} = 0) \ . \qquad (23)$$

Substitution of Equation (23) for the pressure term in I_i results in

$$\frac{1}{V}\int_{S_{sf}} -\, p\, n_i\, dS = \frac{1}{V}\int_{S_{sf}} -\, \tilde{p}\, n_i\, dS + \frac{1}{V}\int_{S_{sf}} -\, p'\, n_i\, dS \qquad (24)$$

The space average pressure, $\tilde{p}$, can be taken outside the integral in Equation (24) and by using Equation (10), Equation (24) can be written as

$$\frac{1}{V}\int_{S_{sf}} -\, p n_i\, dS = \tilde{p}\,\frac{\partial \varepsilon}{\partial y_i} - \frac{1}{V}\int_{S_{sf}} p'\, n_i dS \ . \qquad (25)$$

When similar steps are performed for the viscous stress terms in I_i:

$$I_i = \tilde{p} \frac{\partial \varepsilon}{\partial y_i} - \tilde{\sigma}_{ki} \frac{\partial \varepsilon}{\partial y_k} + \frac{1}{V} \int_{S_{sf}} [- p' n_i + \sigma'_{ik} n_k] dS \ . \tag{26}$$

The first two terms on the right-hand side in Equation (26) are solid-fluid interface forces due to a porosity gradient (analogous to the variable area, one-dimensional flow case) and the third term is the remaining interfacial momentum exchange between the fluid and the embedded stationary surfaces. This latter term is generally expressed in terms of steady state friction factors that are appropriate for the flow field under consideration. In addition to the steady state friction factors, however, flow forces due to transients, such as the added mass (or virtual mass) and Basset forces, are also included in this term. Slattery[14] has applied dimensional analysis to show that steady state momentum exchange may occur due to nonuniform porosity gradients.

Of importance to note is that rigorous evaluation of the integral interfacial momentum exchange would require solutions of the pressure and velocity distributions, so that p' and σ'_{ik} are known, at the interface. In effect, such evaluation would require that the Navier-Stokes equations be solved within the fluid volume. At present, solution of these equations is impractical, and experimental data are required so that algebraic expressions can be substituted for this term.

When Equation (26) is substituted into Equation (22), the result is

$$\frac{\partial}{\partial t} (\varepsilon \tilde{\rho} \tilde{v}_i) + \frac{\partial}{\partial y_k} (\varepsilon \tilde{\rho} \tilde{v}_i \tilde{v}_k) = -\varepsilon \frac{\partial \tilde{p}}{\partial y_i} + \varepsilon \frac{\partial \tilde{\sigma}_{ik}}{\partial y_k} + \varepsilon \tilde{\rho} g_i + F_i + M_i \tag{27}$$

where

$$F_i = \frac{1}{V} \int_{S_{sf}} \left(- p' n_i + \sigma'_{ik} n_k \right) dS \tag{28}$$

and M_i represents the primed terms on the right-hand side of Equation (22). In Equation (27), the average shear stress, is modeled as

$$\tilde{\sigma}_{ik} = - \frac{2}{3} \mu \frac{\partial \tilde{v}_s}{\partial y_s} \delta_{ik} + \mu \left(\frac{\partial \tilde{v}_i}{\partial y_k} + \frac{\partial \tilde{v}_k}{\partial y_i} \right).$$

Modeling of the terms F_i and M_i is discussed in the next section.

3. VOLUME-AVERAGED CONSERVATION OF ENERGY

The fluid average energy equation is obtained by the same process employed in the previous sections.

The local equation for specific internal energy is given by

$$\frac{\partial}{\partial t}\rho I + \frac{\partial}{\partial x_i}\rho v_i I = -\frac{\partial q_i}{\partial x_i} - p d_{ii} + \sigma_{ij} d_{ij} + \rho Q_g \quad . \tag{29}$$

Integration of Equation (29) over V_f, application of Equation (5) to the gadient of q_i, and use of Equation (8) to introduce fluid averages results in

$$\frac{\partial}{\partial t}\widetilde{\varepsilon\rho I} + \frac{\partial}{\partial y_k}\widetilde{\varepsilon\rho v_k I} = -\frac{\partial}{\partial y_k}\varepsilon\tilde{q}_k - \frac{1}{V}\int_{S_{sf}} q_k n_k dS - \frac{1}{V}\int_{V_f} p d_{kk} dV + \frac{1}{V}\int_{V_f}\sigma_{ij} d_{ij} dv + \varepsilon\tilde{\rho}\tilde{Q}_g \quad , \tag{30}$$

where the volumetric energy supply, Q_g, has been assumed constant. Writing the dependent variables as the sum of a spatial average plus a fluctuating part and substituting this sum into Equation (30) gives

$$\frac{\partial}{\partial t}\varepsilon\tilde{\tilde{\rho}}\tilde{\tilde{I}} + \frac{\partial}{\partial y_k}\varepsilon\tilde{\tilde{\rho}}\tilde{\tilde{v}}_k\tilde{\tilde{I}} = -\frac{\partial}{\partial y_k}\varepsilon\tilde{q}_k - \frac{1}{V}\int_{S_{sf}}(\tilde{q}_k + q'_k)n_k dS$$

$$- \frac{1}{V}\int_{V_f}\tilde{\tilde{p}}\tilde{\tilde{d}}_{kk}\, dV - \frac{1}{V}\int_{V_f} p'd'_{kk} dV + \frac{1}{V}\int_{V_f}\tilde{\sigma}_{ij}\tilde{d}_{ij} dV + \frac{1}{V}\int_{V_f}\sigma'_{ij}\, d'_{ij} dV \tag{31}$$

$$+ \varepsilon\tilde{\rho}\tilde{Q}_g - E_i \quad ,$$

where

$$E_i = \frac{\partial}{\partial t}\widetilde{\varepsilon\rho' I'} + \frac{\partial}{\partial y_k}\left[\widetilde{\varepsilon\rho' v'_k I'} + \tilde{\varepsilon\rho}\,\widetilde{v'_k I'} + \varepsilon v_k\widetilde{\rho' I'} + \varepsilon I\widetilde{\rho' v'_k}\right] \quad . \tag{32}$$

Equation (31) can be reduced to a simpler form as follows. The first integral on the right-hand side is evaluated in the same manner as the pressure gradient term in the momentum equation. The results are given by

$$\frac{1}{V}\int_{S_{sf}} (\tilde{q}_k + q'_k) n_k dS = -\tilde{q}_k \frac{\partial \varepsilon}{\partial y_k} - Q_w \tag{33}$$

where

$$Q_w = \frac{1}{V}\int_{S_{sf}} q'_k n_k dS \quad . \tag{34}$$

The third and fourth terms on the right-hand side of Equation (31) represent the change in internal energy of the fluid due to pressure-volume work. The third term is reduced as follows. Writing this term as

$$\frac{1}{V}\int_{v_f} \tilde{\tilde{p}} d_{kk} dV = \frac{1}{V}\int_{v_f} \tilde{p} \widetilde{\frac{\partial v_k}{\partial x_k}} \, dV \tag{35}$$

and taking the spatial averages from under the integral operation gives

$$\frac{1}{V}\int_{v_f} \tilde{p} \widetilde{\frac{\partial v_k}{\partial x_k}} \, dV = \frac{V_f}{V} \tilde{p} \widetilde{\frac{\partial v_k}{\partial x_k}} \quad . \tag{36}$$

When the fluid average definition of Equation (7) is used, Equation (36) can be written as

$$\frac{V_f}{V} \tilde{p} \frac{1}{V_f}\int_{V_f} \frac{\partial v_k}{\partial x_k} dV = \tilde{p} \frac{1}{V}\int_{V_f} \frac{\partial v_k}{\partial x_k} dV \quad , \tag{37}$$

and application of the divergence theorem to the right-hand side gives

$$\tilde{p} \frac{1}{V}\int_{v_f} \frac{\partial v_k}{\partial x_k} dV = \tilde{p} \left[\frac{1}{V}\int_{S_{ff}} v_k n_k dS + \frac{1}{V}\int_{S_{sf}} v_k n_k dS \right] \quad , \tag{38}$$

or, by use of Equations (4), (8), and (9):

$$\tilde{p} \frac{1}{V}\int_{V_f} \frac{\partial v_k}{\partial x_k} dV = \tilde{p} \frac{\partial}{\partial y_k} \varepsilon \tilde{v}_k + \tilde{p} \frac{\partial \varepsilon}{\partial t} \quad . \tag{39}$$

The fourth term on the right-hand side of Equation (31) involves volume averages of fluctuating terms and will be assumed to be small compared to the other terms in the energy equation.

The fifth and sixth terms on the right-hand side of Equation (31) represent the change in internal energy of the fluid due to viscous dissipation. Since viscous dissipation is usually neglected in applications of the local equations, these volume integrals will also be assumed small compared to internal energy changes due to energy exchanges related to temperature differences between the fluid and solid; that is:

$$\frac{1}{V}\int_{V_f} \tilde{\sigma}_{ij}\,\tilde{d}_{ij}\,dV \simeq 0 \tag{40}$$

and

$$\frac{1}{V}\int_{V_f} \widetilde{\sigma'_{ij}\,d'_{ij}}\,dV \simeq 0\ . \tag{41}$$

The final formulation of the volume-averaged energy equation is obtained by substituting the results of Equations (33) and (39) through (41) into Equation (31) to obtain

$$\frac{\partial}{\partial t}\,\varepsilon\rho\tilde{\tilde{I}} + \frac{\partial}{\partial y_k}\,\varepsilon\rho\tilde{\tilde{v}}_k\tilde{I} = -\,\varepsilon\frac{\partial}{\partial y_k}\,\tilde{q}_k - \tilde{p}\frac{\partial}{\partial y_k}\,\varepsilon\tilde{v}_k - \tilde{p}\frac{\partial\varepsilon}{\partial t} + \varepsilon\rho\tilde{Q}_g + Q_w - E_i \tag{42}$$

where E_i is given by Equation (32). The average molecular heat conduction, $\tilde{q}_k$, in Equation (42) is modeled as

$$\tilde{q}_k = -k\,\frac{\partial T}{\partial y_k}\ . \tag{43}$$

4. STATE EQUATION

The state equation is used with density as a function of the independent variables pressure and internal energy. This form of the state equation is chosen because of the nearly incompressible character of subcooled water. The local state equation can be written as

$$\rho = f\,(p,I)\ . \tag{44}$$

Integration of Equation (44) over V_f gives

$$\tilde{\rho} = \widetilde{f\ (p,I)}\ . \tag{45}$$

Expansion of the response function f in a Taylor series about $(\tilde{p},\tilde{I})$ results in

$$f\ (p,I) = f\ (\tilde{p},\tilde{I}) + \frac{\partial f}{\partial p}\ (\tilde{p},\tilde{I})\ p' + \frac{\partial f}{\partial I}\ (\tilde{p},\tilde{I})\ I' + \ldots \tag{46}$$

Substitution of Equation (46) into Equation (45) results in

$$\tilde{\rho} = f\ (\tilde{p},\tilde{I}) \tag{47}$$

if averages of the products of fluctuating variables are neglected.

III. CLOSURE OF THE EQUATION SYSTEM

Use of the volume-averaging procedure given in the previous section has introduced several unknowns. Most of these are analogous to quantities that are introduced when the three-dimensional local equations are averaged to obtain the one-dimensional equations usually employed in engineering analyses. However, treatment of these quantities in the volume-averaged three-dimensional equations will require additional considerations. The purpose of the present section is to present a discussion of these quantities. Specific models will not be given because the purpose of the present report is to present the general formulation of the equations. In addition, different applications of the formulation may require different specific relations, all of which can not be covered here.

The quantities introduced by the volume-averaging procedure are summarized for convenience.

The conservation of mass equation, Equation (17), contains the term

$$\frac{\partial}{\partial y_k} \left(\varepsilon \widetilde{\rho' v_k'}\right) \quad , \tag{48}$$

which has been assumed to be small.

The linear momentum balance, Equation (27), contains the fluid-solid momentum exchange of Equation (28):

$$F_i = \frac{1}{V} \int_{S_{ff}} \left[- p' n_i + \sigma_{ik}' n_k \right] dS \quad , \tag{49}$$

and the terms of Equation (22) due to spatial nonuniformity:

$$M_i = \frac{\partial}{\partial t} \widetilde{\varepsilon \rho' v_i'} + \frac{\partial}{\partial y_k} \left[\left(\varepsilon \tilde{\rho} \widetilde{v_i' v_k'}\right) + \left(\varepsilon \tilde{v}_i \widetilde{\rho' v_k'}\right) + \left(\varepsilon \tilde{v}_k \widetilde{\rho' v_i'}\right) + \widetilde{\varepsilon \rho' v_i' v_k'} \right] . \tag{50}$$

The internal energy equation, Equation (42), contains the fluid-solid energy exchange of Equation (34):

$$Q_w = \frac{1}{V} \int_{S_{sf}} q_k' n_k dS \quad , \tag{51}$$

and the terms of Equation (32) due to spatial nonuniformity:

$$E_i = \frac{\partial}{\partial t} \widetilde{\varepsilon \rho' I'} + \frac{\partial}{\partial y_k} \left[\widetilde{\varepsilon \rho' v_k' I'} + \widetilde{\varepsilon \rho v_k' I'} + \widetilde{\varepsilon v_k \rho' I'} + \widetilde{\varepsilon I \rho' v_k'} \right] . \tag{52}$$

Several other terms introduced into the energy equation by the averaging process have been neglected as indicated in Section II-3.

The equation development given in Section II was quite general so that most of the assumptions associated with the general formulation will be invoked in evaluation of Equations (49) through (52). Many expressions are available for these terms for the case of single-phase flows in a wide variety of geometries. However, the primary area of application of the model of interest to the nuclear industry, that is, to thermal-hydraulic analysis of fuel rod arrays, introduces several difficulties. The two major difficulties are (1) existence of two-phase flow structure and (2) lack of comprehensive data for heat transfer in nonparallel flows. These subjects will be discussed in this section along with the general requirements for closure of the equation system.

1. FLUID-SOLID INTERFACIAL MOMENTUM EXCHANGE

The interfacial momentum exchange is given by Equation (49). As previously discussed, rigorous evaluation of this term would require that the detailed pressure and velocity distributions be known within the fluid. However, since obtaining these distributions is not practical at this time (although analytical solutions for simple physical approximations to the real situation can prove useful), real engineering flows must be analyzed by use of empirical correlations. To improve confidence in results obtained from the general model formulation, correlations that have been derived from data that correspond to the area of application should be used.

The momentum exchange is expressed in terms of friction factors as follows. The argument of the integral in Equation (49) is taken as some representative average value so that Equation (49) can be written as

$$\frac{1}{V}\int_{S_{sf}}\left[-p'n_i+\sigma'_{ik}n_k\right]dS=\frac{S_{sf}}{V}\,B_w^{ij}\tilde{v}_j\quad. \tag{53}$$

If the solids in the core have orthotropic symmetry, then $B_w^{ij}=0$ when $i\neq j$. Orthotropic symmetry is assumed in the following. The nonzero B_w^{ij} in this case are functions of (v_1^2, v_2^2, v_3^2) and scalars characterizing the fluid properties and geometry of the solids. By letting S_{sf}/V be denoted by A_w, the wetted wall surface area per unit volume, and by substituting Equation (53) into Equation (49), the following is obtained:

$$F_i=A_wB_w^{ij}\tilde{v}_j\quad(B_w^{ij}=0,i\neq j)\quad. \tag{54}$$

Although in general the momentum exchange may include transient effects, only the steady state contribution will be discussed here. The quantity B_w^{ij} in Equation (54) is given by[a]

$$B_w^{ii} = \frac{1}{8} \tilde{\rho} \left| \tilde{v}_i \right| f_w^i \tag{55}$$

where f_w^i is the friction factor and $|\tilde{v}_i|$ is the speed in the i direction.

A great deal of experimental effort has been devoted to determine the functional dependency of f_w^i on fluid and flow field properties. A general relationship can be written

$$f_w^i = Q^i \left(Re_w^i, \varepsilon, \text{other geometric factors} \right) \tag{56}$$

where the Reynolds number is given by

$$Re_w^i = \frac{\varepsilon 4 \left| \tilde{v}_i \right| \tilde{\rho}}{\mu A_w} \tag{57}$$

and the speed in the i^{th} direction is given by

$$\left| \tilde{v}_i \right| = (v_i v_i)^{1/2} \qquad \text{(no sum on i)} \tag{58}$$

The operational equation for f_w^i as shown by Equation (56), depends on the geometry of the solid-fluid interfaces embedded in the flow field, and many general expressions have been generated from analysis of experimental data. These may be summarized as follows for parallel flows. For laminar, or slow, flows:

$$f_w^i = C_1 / Re_w^i \tag{59}$$

and for turbulent, or high speed, flows:

$$f_w^i = C_2 \left(Re_w^i \right)^n + C_3 \tag{60}$$

---

[a] This form for B_w^{ij} is limited to geometries for which three perpendicular directions can be found along which the imbedded surfaces resist the fluid motion but do not change the direction of the fluid. The form for B_w^{ij} is given in these coordinates.

Other invariant forms for B_w^{ij} could be given. B_w^{ij} could be modeled as dependent upon the total velocity $| \underset{\sim}{v} | = (\sum_{i=i}^{3} \tilde{v}_i \tilde{v}_i)^{1/2}$ instead of velocity components $|\tilde{v}_i|$. A B_w^{ij} form, which was dependent on the total velocity, did not compare with data as well as Equation (55).

or

$$\frac{1}{\sqrt{f_w^{\,i}}} = C_4 \log \left(Re_w^{\,i} \sqrt{f_w^{\,i}}\right) + C_5 \quad . \tag{61}$$

The last equation, which can be modified to include wall roughness effects, gives better agreement with data over a wider range of flow speeds than Equation (60).

The constants in Equations (59) through (61), C_1 through C_5, and n have been determined for a number of rod array configurations[15-22]. For flows in porous media and fluidized-bed flows, the constants C_1, C_2, C_3, and C_4 usually become functions of the porosity, ϵ. Expressions for friction forces for flows normal to rod arrays can be obtained from References 23 through 27.

1.1 Friction Multipliers for Two-Phase Flow

When the fluid in the flow field is present as two phases instead of one, the modeling of Equations (49) through (52) may be changed. Most current two-phase flow analysis methods incorporate changes in the models. As an example of this modeling, the momentum exchange F_i of Equation (49) will be considered.

Combining Equation (55) with Equation (54) gives

$$F_i = \frac{1}{8} A_w \tilde{\rho} \tilde{v}_i \left|\tilde{v}_i\right| f_w^{\,i} \quad . \tag{62}$$

The two-phase multiplier is the ratio between the frictional pressure gradient for the two-phase flow and the frictional pressure gradient for related single-phase flows. For example, if the two-phase mixture is of low quality, the friction factor may be taken as that obtained if the total flow (liquid plus vapor) flowed entirely as liquid. Then Equation (62) can be written

$$\frac{1}{8} f_w^{\,i} A_w \tilde{\rho} \left|\tilde{v}_i\right| \tilde{v}_i = \frac{1}{8} f_{w_{\ell o}}^{\,i} A_w \phi_{\ell o}^2 \tilde{\rho}_\ell \left|\tilde{v}_i^{\ell}\right| \tilde{v}_i^{\ell} \tag{63}$$

where $\phi_{\ell o}^2$ is the two-phase multiplier and the velocity $\tilde{v}_i^{\ell}$ is

$$\tilde{v}_i^{\ell} = \frac{\tilde{\rho}\, \tilde{v}_i}{\tilde{\rho}_\ell} \quad . \tag{64}$$

The appropriate Reynolds number is given by

$$Re_w^{\,i} = \frac{\varepsilon 4 \tilde{\rho}_\ell \left|\tilde{v}_i^{\ell}\right|}{\mu_\ell A_w} \quad . \tag{65}$$

For this case, $\phi_{\ell o}^2$ in Equation (63) becomes

$$\phi_{\ell o}^2 = 1 + x\left(\frac{\tilde{\rho}_\ell}{\tilde{\rho}_g} - 1\right) \quad . \tag{66}$$

A wide variety of two-phase multiplier models have appeared in the literature. For example, different definitions of the mixture viscosity can be used in the Reynolds number of Equation (65) with $\phi_{\ell o}^2$ correspondingly changed. Or, for high quality flows, the reference frictional pressure gradient can be taken to be that for the case of only vapor present. Additional two-phase friction multipliers are available from References 28 through 34. Among the more interesting approaches are those of Beattie[29,30] who has considered the effect of flow regimes and that of Lombardi and Pedrocchi[34] who have directly correlated data without using a two-phase multiplier.

1.2 Vapor Volume Fraction and Velocity Slip Ratio

Some of the two-phase friction multipliers discussed previously require the vapor volume fraction, or void fraction, and the vapor velocity-liquid velocity ratio, or slip ratio. These two quantities can also be used to modify the time and space derivatives on the left-hand side of Equations (18), (27), and (42) in order to account for some two-phase fluid effects. Void fraction and slip ratio correlations are available from References 28, 33, and 35 through 41.

2. SPATIALLY NONUNIFORM VELOCITY FLUCTUATION

Contributions due to spatially nonuniform velocity fluctuations are given by Equation (50) and represent contributions to the momentum balance due to curved streamlines within the flow field. If the terms containing ρ' are assumed small compared to the other terms, Equation (50) becomes

$$M_i = \frac{\partial}{\partial y_k} \varepsilon \tilde{\rho} \widetilde{v_i' v_k'} \quad . \tag{67}$$

This term, which is analogous to Reynolds' stress terms when time averaging is employed, will be assumed to have the form of an additional stress which acts as an effective increase in the viscosity of the fluid. The average of the product of the fluctuating terms can then be written as

$$\varepsilon \widetilde{\rho v_i' v_k'} = \varepsilon \left[-\frac{2}{3} \mu_t \frac{\partial \tilde{v}_s}{\partial y_s} \delta_{ik} + \mu_t \left(\frac{\partial \tilde{v}_i}{\partial y_k} + \frac{\partial \tilde{v}_k}{\partial y_i} \right) \right] \tag{68}$$

where μ_t is the turbulent viscosity.

All existing one-dimensional rod array analysis codes contain models for the turbulent viscosity and many experimental and analytical investigations have been conducted in order to determine its value. Among the more recent of these are the work of Rowe[42] and Rowe and Chapman[43]. Reviews of the models available prior to 1972 have been given by Rogers and Rosehart[44] and Galbraith and Knudsen[45]. Kjellestrom[46, 47] has also measured turbulence properties in rod array subchannels and evaluated correlation models against data. The experimental work of Rowe and Kjellestrom is expected to contribute significantly toward resolution of modeling questions associated with turbulent flows in the geometrically complex rod array subchannel. In particular, modeling based on "universal" velocity distributions taken from simple channels will no longer be necessary.

Most expressions for μ_t can be written in the form

$$\frac{\mu_t}{\mu} = C_6 \, Re_w \sqrt{\frac{f_i}{2}} \tag{69}$$

or

$$\frac{\mu_t}{\mu} = C_7 \, Re_w^m \tag{70}$$

Equations (69) and (70) are flow channel average values. The effects of the presence of two phases on μ_t is not well known. Beattie[48] has given a simple preliminary model.

3. FLUID-SOLID INTERFACIAL ENERGY EXCHANGE

The fluid-solid interfacial energy exchange is given by Equation (51) and may be obtained by either of two methods as follows: (1) the fluid-solid heat flux may be prescribed as a function of (x, y, z, t), or (2) the interfacial surface temperature may be prescribed (or calculated) and the energy exchange determined from correlations relating the heat transfer to the fluid-solid temperature difference. For nuclear reactor thermal-hydraulic analysis, the latter is usually necessary.

Equation (51) may be evaluated in a manner similar to evaluation of Equation (53) in Section III-1. The results are given by

$$Q_w = A_h h \, (T_s - T_b) \tag{71}$$

where A_h is the heated area per unit volume, h is a heat transfer coefficient, T_s is the surface temperature, and T_b is the bulk temperature of the fluid. Correlations for h and for departure from nucleate boiling (DNB) are available from References 49 through 51.

4. SPATIALLY NONUNIFORM ENERGY FLUCTUATIONS

Terms for spatially nonuniform energy fluctuations are given in Equation (52) and represent energy exchange due to the spatially nonuniform distribution of energy within the flow field. Again, evaluation is similar to that of the momentum terms in Section III-2. The contribution from ρ' is considered small so that Equation (52) can be written

$$E_i = \frac{\partial}{\partial y_k} \widetilde{\varepsilon\rho v_k' I'} \tag{72}$$

where

$$\widetilde{\varepsilon\rho v_k' I'} = -\varepsilon\rho k_t \frac{\partial}{\partial y_k} \tilde{I} \quad . \tag{73}$$

The turbulent thermal coefficient, k_t, can be obtained from correlations of the form

$$\frac{k_t}{k/\rho C_p} = C_8 \, Re_w \sqrt{\frac{f_w}{2}} \, Pr \tag{74}$$

or

$$\frac{k_t}{k/\rho C_p} = C_9 \, Re_w^q \, Pr^r \tag{75}$$

where the constants C_8, C_9, q, and r are determined from experimental data. As in the case of momentum, Equations (74) and (75) are flow channel average values that do not consider the local details of the turbulence.

5. FINAL FORM OF THE EQUATIONS

The final form of the equations is obtained by substituting the modeling equations from Sections III-1 through III-4 into the averaged equations from Section II. The results are summarized here for convenience:

The conservation of mass equation is

$$\frac{\partial}{\partial t} \varepsilon\tilde{\rho} + \frac{\partial}{\partial y_k} \varepsilon\tilde{\rho}\tilde{v}_k = 0 \quad . \tag{76}$$

The linear momentum balance is

$$\frac{\partial}{\partial t} \varepsilon\tilde{\rho}\tilde{v}_i + \frac{\partial}{\partial y_k} \varepsilon\tilde{\rho}\tilde{v}_i\tilde{v}_k = -\varepsilon \frac{\partial p}{\partial y_i} + \varepsilon \frac{\partial}{\partial y_k} \tilde{\sigma}_{ik} + \frac{\partial}{\partial y_k} \varepsilon\rho\sigma_{ik}^T + F_i + \varepsilon\tilde{\rho}g_i \tag{77}$$

where

$$\sigma_{ik}^{T} = -\frac{2}{3}\,\nu_t\,\frac{\partial \tilde{v}_s}{\partial y_s}\,\delta_{ik} + \nu_t\left(\frac{\partial \tilde{v}_i}{\partial y_k} + \frac{\partial \tilde{v}_k}{\partial y_i}\right). \tag{78}$$

The conservation of energy equation is

$$\frac{\partial}{\partial t}\,\varepsilon\tilde{\rho}\tilde{\tilde{I}} + \frac{\partial}{\partial y_k}\,\varepsilon\tilde{\rho}\tilde{\tilde{I}}\tilde{v}_k = \varepsilon\,\frac{\partial}{\partial y_k}\left(k\,\frac{\partial \tilde{T}}{\partial y_k}\right) + \frac{\partial}{\partial y_k}\left(\varepsilon\rho k_t\,\frac{\partial \tilde{I}}{\partial y_k}\right) \tag{79}$$

$$-\tilde{p}\,\frac{\partial}{\partial y_k}\,\varepsilon\tilde{v}_k - \tilde{p}\,\frac{\partial \varepsilon}{\partial t} + Q_w + \varepsilon\tilde{\rho}Q_g \quad .$$

IV. NUMERICAL TECHNIQUE

The numerical technique used to solve Equations (76) through (79) is based on the MAC method for incompressible flow as modified by Hirt and Cook[52] and the ICE technique for compressible flow[53]. The essential features of these two methods are: (1) the continuity equation is implicit in density and velocity, (2) the linear momentum equation is implicit in pressure, and (3) the energy equation is purely explicit.

1. BASIC SCHEME

For convenience, the momentum equation for compressible flow is written in a form compatible with the incompressible MAC technique so that Equation (77) becomes

$$\frac{\partial \tilde{v}_i}{\partial t} + \frac{\partial (\tilde{v}_i \tilde{v}_k)}{\partial y_k} = -\frac{1}{\tilde{\rho}} \frac{\partial \tilde{p}}{\partial y_i} + \tilde{v}_i \frac{\partial \tilde{v}_k}{\partial y_k}$$

$$+ \frac{1}{\tilde{\rho}} (\mu + \mu_t) \frac{\partial^2 \tilde{v}_i}{\partial y_k \partial y_k} + \frac{1}{3\tilde{\rho}} (\mu + \mu_t) \frac{\partial}{\partial y_i} \left(\frac{\partial \tilde{v}_k}{\partial y_k} \right) \tag{80}$$

$$+ F_i / \epsilon \tilde{\rho} + g_i \quad .$$

For the stress terms in Equation (80), μ, μ_t, and ϵ have been assumed to vary slowly in space and are taken outside the spatial derivatives.

The region in which computations are to be performed is divided into a set of small rectangular cells of size Δx_i, Δy_j, and Δz_k. As shown in Figure 2, velocity components are located at cell faces; and density, specific internal energy, and pressure are located at cell centers. Cells are labeled with the index (i, j, k) as counted from the origin in the x, y, z directions, respectively. A time-dependent solution is obtained by expressing Equations (76) through (79) in finite difference form and advancing the variables through a sequence of short time steps of duration Δt. The advancement for each time step is accomplished in two stages. In the first stage, all quantities are advanced purely explicitly. These quantities then provide the initial estimates for stage two in which the implicit quantities are obtained by means of a cell-by-cell interation process.

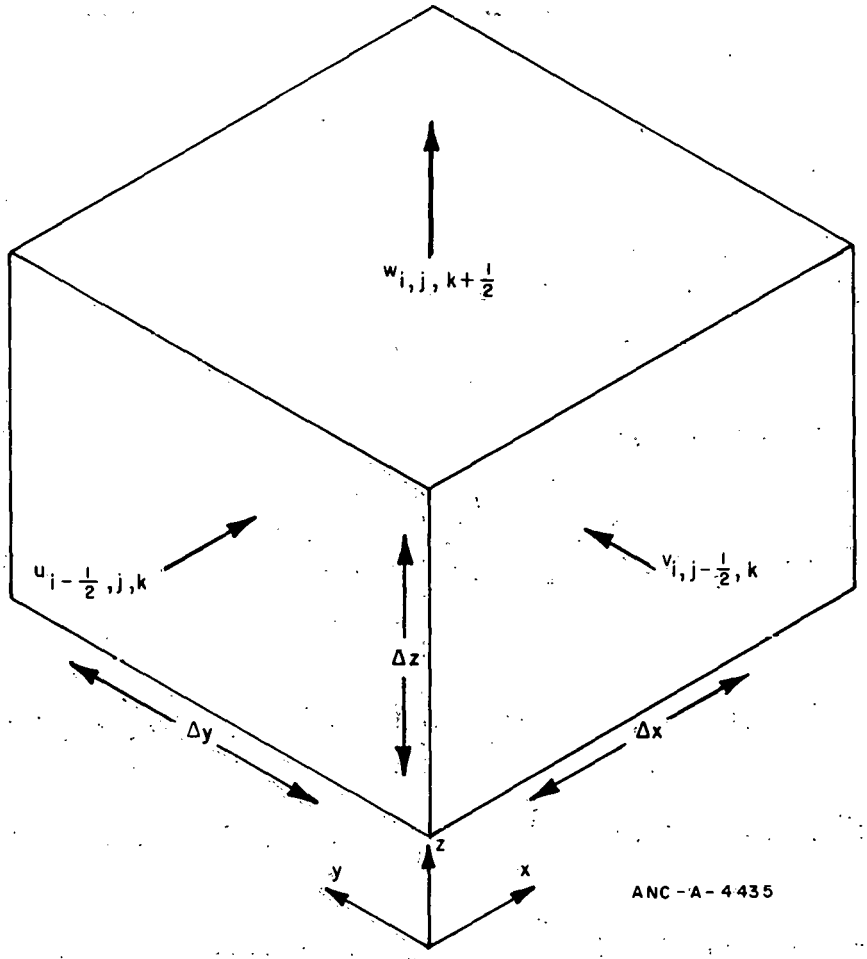

Fig. 2 The computational cell.

The specific finite difference equations used are:

(1) The mass conservation equation:

$$(\varepsilon\rho)^{n+1}_{ijk} = (\varepsilon\rho)^{n}_{ijk} + \frac{\Delta t}{2}\left\{\left[u^{n+1}_{i-1/2jk}\left[(\varepsilon\rho)^{n+1}_{i-1jk} + (\varepsilon\rho)^{n+1}_{ijk}\right]\right.\right.$$

$$+ \alpha_x\left|u^{n+1}_{i-1/2jk}\right|\left[(\varepsilon\rho)^{n+1}_{i-1jk} - (\varepsilon\rho)^{n+1}_{ijk}\right] - u^{n+1}_{i+1/2jk}\left[(\varepsilon\rho)^{n+1}_{ijk} + (\varepsilon\rho)^{n+1}_{i+1jk}\right]$$

$$\left.\left. - \alpha_x\left|u^{n+1}_{i+1/2jk}\right|\left[(\varepsilon\rho)^{n+1}_{ijk} - (\varepsilon\rho)^{n+1}_{i+1jk}\right]\right]/\Delta x_i + \left[v^{n+1}_{ij-1/2k}\cdot\left[(\varepsilon\rho)^{n+1}_{ij-1k} + (\varepsilon\rho)^{n+1}_{ijk}\right]\right.$$

$$\left. + \alpha_y\left|v^{n+1}_{ij-1/2k}\right|\left[(\varepsilon\rho)^{n+1}_{ij-1k} - (\varepsilon\rho)^{n+1}_{ijk}\right] - v^{n+1}_{ij+1/2k}\left[(\varepsilon\rho)^{n+1}_{ijk} + (\varepsilon\rho)^{n+1}_{ij+1k}\right]\right.$$

$$- \alpha_y \left| v^{n+1}_{ij+1/2k} \right| \left[(\varepsilon\rho)^{n+1}_{ijk} - (\varepsilon\rho)^{n+1}_{ij+1k} \right] \Big] / \Delta y_j + \Big[w^{n+1}_{ijk-1/2} \left[(\varepsilon\rho)^{n+1}_{ijk-1} + (\varepsilon\rho)^{n+1}_{ijk} \right]$$

$$+ \alpha_z \left| w^{n+1}_{ijk-1/2} \right| \cdot \left[(\varepsilon\rho)^{n+1}_{ijk-1} - (\varepsilon\rho)^{n+1}_{ijk} \right] - w^{n+1}_{ijk+1/2} \left[(\varepsilon\rho)^{n+1}_{ijk} + (\varepsilon\rho)^{n+1}_{ijk+1} \right]$$

$$- \alpha_z \left| w^{n+1}_{ijk+1/2} \right| \left[(\varepsilon\rho)^{n+1}_{ijk} - (\varepsilon\rho)^{n+1}_{ijk+1} \right] \Big] / \Delta z_k \Big\} \qquad (81)$$

(2) The linear momentum equation:

$$u^{n+1}_{i+1/2jk} = u_{i+1/2jk} - \frac{2\Delta t}{\left(\Delta x_i + \Delta x_{i+1} \right)} \frac{\left(p^{n+1}_{ijk} - p^{n+1}_{i+1jk} \right)}{\left((\varepsilon\rho)_{i+1/2jk} \right)} \varepsilon_{i+1/2jk} + \Delta t g_x \cdot$$

$$- \Delta t F^x_{i+1/2jk} / \quad (\varepsilon\rho)_{i+1/2jk} \quad - \frac{\Delta t}{(\Delta x_i + \Delta x_{i+1})} \Big[u_{i+1jk} \left(u_{i+1/2jk} + u_{i+3/2jk} \right)$$

$$+ \alpha_x \left| u_{i+1jk} \right| \left(u_{i+1/2jk} - u_{i+3/2jk} \right) - u_{ijk} \left(u_{i-1/2jk} + u_{i+1/2jk} \right) - \alpha_x \left| u_{ijk} \right| \cdot$$

$$\left(u_{i-1/2jk} - u_{i+1/2jk} \right) \Big] - \frac{\Delta t}{2\Delta y_j} \Big[v_{i+1/2j+1/2k} \left(u_{i+1/2jk} + u_{i+1/2j+1k} \right)$$

$$+ \alpha_y \left| v_{i+1/2j+1/2k} \right| \cdot \left(u_{i+1/2jk} - u_{i+1/2jk+1k} \right) - v_{i+1/2j-1/2k}$$

$$\left(u_{i+1/2j-1k} + u_{i+1/2jk} \right) - \alpha_y \left| v_{i+1/2j-1/2k} \right| \cdot \left(u_{i+1/2j-1k} - u_{i+1/2jk} \right) \Big]$$

$$- \frac{\Delta t}{2\Delta z_k} \Big[w_{i+1/2jk+1/2} \left(u_{i+1/2jk} + u_{i+1/2jk+1} \right) + \alpha_z \left| w_{i+1/2jk+1/2} \right|$$

$$\left(u_{i+1/2jk} - u_{i+1/2jk+1} \right) - w_{i+1/2jk-1/2} \left(u_{i+1/2jk-1} + u_{i+1/2jk} \right) -$$

$$\alpha_z \left| w_{i+1/2jk-1/2} \right| \left(u_{i+1/2jk-1} - u_{i+1/2jk} \right) \Big]$$

$$+\frac{\Delta t}{\Delta x_i}\left[u_{i+1/2jk}\left(u_{i+1jk}-u_{ijk}\right)\right]+\frac{\Delta t}{\Delta y_j}\left[u_{i+1/2jk}\left(v_{i+1/2j+1/2k}-v_{i+1/2j-1/2k}\right)\right]$$

$$+\frac{\Delta t}{\Delta z_k}\left[u_{i+jk}\left(w_{i+1/2jk+1/2}-w_{i+1/2jk-1/2}\right)\right]+\Delta t+\frac{\varepsilon_{i+1/2jk}\,(\mu+\mu_T)_{i+1/2jk}\Delta t}{(\varepsilon\rho)_{i+1/2jk}}$$

$$\left[(\nabla^2 u)_{i+1/2jk}+\frac{2}{3}\,\frac{(\nabla\cdot u)_{i+1jk}-(\nabla\cdot u)_{ijk}}{\Delta x_i+\Delta x_{i+1}}\right] \tag{82}$$

where

$$\left(\nabla^2 u\right)_{i+1/2jk}=2\left[\left(u_{i+3/2jk}-u_{i+1/2jk}\right)/\Delta x_{i+1}-\left(u_{i+1/2jk}+u_{i-1/2jk}\right)/\Delta x_i\right]$$

$$/\left(\Delta x_i+\Delta x_{i+1}\right)+\left[2\left(u_{i+1/2j+1k}-u_{i+1/2jk}\right)/\left(\Delta y_j+\Delta y_{j+1}\right)\right.$$

$$\left.-2\left(u_{i+1/2jk}-u_{i+1/2j-1k}\right)/\left(\Delta y_j+\Delta y_{j-1}\right)\right]/\Delta y_j+\left[2\left(u_{i+1/2jk+1}-u_{i+1/2jk}\right)\right.$$

$$\left./\left(\Delta z_k+\Delta z_{k+1}\right)-2\left(u_{i+1/2jk}-u_{i+1/2jk-1}\right)/\left(\Delta z_k+\Delta z_{k-1}\right)\right]/\Delta z_k \tag{83}$$

and

$$\left(\nabla\cdot u\right)_{ijk}=\frac{u_{i+1/2jk}-u_{i-1/2jk}}{\Delta x_i}+\frac{v_{ij+1/2k}-v_{ij-1/2k}}{\Delta y_j}+\frac{w_{ijk+1/2}-w_{ijk-1/2}}{\Delta z_k}$$

with similar linear momentum equations for the y and z directions.

(3) The energy equation:

$$\left(\varepsilon\rho\right)_{ijk}\,I_{ijk}^{n+1}=(\varepsilon\rho)_{ijk}\,I_{ijk}+\frac{(\varepsilon\rho)_{ijk}\,\Delta t}{2}\left\{\left[u_{i-1/2jk}\left(I_{i-1jk}+I_{ijk}\right)\right.\right.$$

$$\left.+\alpha'_x\left|u_{i-1/2jk}\right|\left(I_{i-1jk}-I_{ijk}\right)-u_{i+1/2jk}\left(I_{ijk}+I_{i+1jk}\right)-\alpha'_x\left|u_{i+1/2jk}\right|\right.$$

$$\left(I_{ijk} - I_{i+1jk}\right)\Big] / \Delta x_i + \Big[v_{ij-1/2k} \cdot \left(I_{ij-1k} + I_{ijk}\right) + \alpha'_y \left| v_{ij-1/2k} \right|$$

$$\left(I_{ij-1k} - I_{ijk}\right) - v_{ij+1/2k} \left(I_{ijk} + I_{ij+1k}\right) - \alpha'_y \left| v_{ij+1/2k} \right| \left(I_{ijk} - I_{ij+1k}\right)\Big] / \Delta y_j$$

$$+ \Big[w_{ijk-1/2} \left(I_{ijk-1} + I_{ijk}\right) + \alpha'_z \left| w_{ijk-1/2} \right| \cdot \left(I_{ijk-1} - I_{ijk}\right)$$

$$- w_{ijk+1/2} \left(I_{ijk} + I_{ijk+1}\right) - \alpha'_z \left| w_{ijk+1/2} \right| \left(I_{ijk} - I_{ijk+1}\right)\Big] / \Delta z_k \Big\}$$

$$+ \Delta t \left[(\varepsilon\rho)_{ijk} I_{ijk} - p_{ijk} \varepsilon_{ijk}\right] \left[\frac{u_{i+1/2jk} - u_{i-1/2jk}}{\Delta x_i} + \frac{v_{ij+1/2k} - v_{ij-1/2k}}{\Delta y_j}\right.$$

$$\left. + \frac{w_{ijk+1/2} - w_{ijk-1/2}}{\Delta z_k}\right] + \Delta t k_T \Big\{\Big[2(\varepsilon\rho)_{i+1/2jk} \left(I_{i+1jk} - I_{ijk}\right)$$

$$/ \left(\Delta x_i + \Delta x_{i+1}\right) - 2(\varepsilon\rho)_{i-1/2jk} \left(I_{ijk} - I_{i-1jk}\right) / \left(\Delta x_i + \Delta x_{i-1}\right)\Big] / \Delta x_i$$

$$+ \Big[2(\varepsilon\rho)_{ij+1/2k} \left(I_{ij+1k} - I_{ijk}\right) / \left(\Delta y_j + \Delta y_{j+1}\right) - 2(\varepsilon\rho)_{ij-1/2k} \left(I_{ijk} - I_{ij-1k}\right)$$

$$/ \left(\Delta y_j + \Delta y_{j-1}\right)\Big] / \Delta y_j + \Big[2(\varepsilon\rho)_{ijk+1/2} \left(I_{ijk+1} - I_{ijk}\right) / \left(\Delta z_k + \Delta z_{k+1}\right)$$

$$- 2(\varepsilon\rho)_{ijk-1/2} \left(I_{ijk} - I_{ijk-1}\right) / \left(\Delta z_k + \Delta z_{k-1}\right)\Big] / \Delta z_k \Big\} + Q^w_{ijk} + (\varepsilon\rho)_{ijk} Q_{g_{ijk}}$$

(85)

where, for convenience, the volume average symbol ¯ has been omitted, and the velocity components are denoted by u, v, w. The superscript n + 1 denotes an advanced time quantity, whereas no superscript denotes the previous time values of any quantity. In Equations (81) through (85), the donor cell and centered finite differencing have been combined so that α_i=1 (or α'_i) yields full donor cell differencing, and α_i=0 yields centered

differencing. Quantities required at positions other than where they are defined are calculated as simple averages; for example, $u_{ijk} = (u_{i+1/2jk} + u_{i-1/2jk})/2$. For the pressure volume-change terms in Equation (85), ϵ has been assumed to vary slowly and its space and time derivatives have been neglected.

To obtain the implicit character described, the following cell-by-cell calculational procedure is used:

(1) The advanced time specific internal energies are calculated according to Equation (85).

(2) The tentative advanced time velocities for each cell are calculated according to Equation (82) and the corresponding equations for v and w, etc., using the previous time pressures.

(3) The tentative advanced time pressure is calculated such that the pressure change in each cell is proportional to the excess mass that accumulates in the cell beyond that consistent with mass conservation; that is:

$$p^{n+1}_{ijk} = \hat{p}_{ijk} + \delta p_{ijk} \tag{86}$$

where

$$\delta p_{ijk} = -\Delta\tau S_{ijk} \tag{87}$$

$$S_{ijk} = \frac{\hat{\rho}_{ijk} - \rho^{n}_{ijk}}{\Delta t} + \left[\frac{\partial \hat{\rho}\, \hat{v}_k}{\partial x_k}\right]_{ijk}$$

and $\hat{}$ denotes the most recent tentative advanced time quantity, and the divergence term is differenced as in Equation (81). For the first iteration of any time step, $\hat{\rho}$ is calculated as

$$\hat{\rho} = f\left(p^{n}, I^{n+1}\right) \tag{88}$$

(4) The new advanced velocities are then calculated from the new pressures by

$$u^{n+1}_{i+1/2k} = \hat{u}_{i+1/2jk} + \frac{2\Delta t}{\left(\Delta x_i + \Delta x_{i+1}\right)} \frac{\epsilon_{i+1/2jk}\, \delta p_{ijk}}{\left((\epsilon\rho)^{n}_{i+1/2jk}\right)}$$

$$u^{n+1}_{i-1/2jk} = \hat{u}_{i-1/2jk} - \frac{2\Delta t}{\left(\Delta x_i + \Delta x_{i-1}\right)} \frac{\epsilon_{i-1/2jk}\, \delta p_{ijk}}{\left((\epsilon\rho)^{n}_{i-1/2jk}\right)}$$

$$v^{n+1}_{ij+1/2k} = \hat{v}_{ij+1/2k} + \frac{2\Delta t}{\left(\Delta y_j + \Delta y_{j+1}\right)} \frac{\epsilon_{ij+1/2k}\, \delta p_{ijk}}{\left((\epsilon\rho)^{n}_{ij+1/2k}\right)}$$

$$v^{n+1}_{ij-1/2k} = \hat{v}_{ij-1/2k} - \frac{2\Delta t}{\left(\Delta y_j + \Delta y_{j-1}\right)} \frac{\varepsilon_{ij-1/2k}\ \delta p_{ijk}}{\left((\varepsilon\rho)^n_{ijk-1/2}\right)}$$

$$w^{n+1}_{ijk+1/2} = \hat{w}_{ijk+1/2} + \frac{2\Delta t}{\left(\Delta z_k + \Delta z_{k+1}\right)} \frac{\varepsilon_{ijk+1/2}\ \delta p_{ijk}}{\left((\varepsilon\rho)^n_{ijk+1/2}\right)} \cdot$$

$$w^{n+1}_{ijk-1/2} = w_{ijk-1/2} - \frac{2\Delta t}{z_k + z_{k-1}} \frac{\varepsilon_{ijk-1/2}\ \delta p_{ijk}}{(\varepsilon\rho)^n_{ijk-1/2}} \cdot \tag{89}$$

Equation (89) is evaluated for each cell in turn using the previous velocity iterates on the right, front, and top faces and the new velocity iterates on the left, back, and bottom faces so that the velocity on a face is modified due to the pressure changes in the two adjacent cells. The mesh is swept successively in the direction of increasing j for each (i, k) plane and in the direction of increasing k for each i column. Viecelli[54] has shown that this type of procedure is equivalent to successive overrelaxation and is superior to simply using the previous iterates.

(5) The new tentative advanced time densities for each cell are then calculated from the equation of state in the form $\rho = f(p, I)$ using the most recent value of p. Alternately, the linearized equation of state $\overline{\delta\rho} = \delta\overline{p}/C_I^2$ may be used, where C_I is the sound speed at constant internal energy.

(6) Steps 3 through 5 are repeated until the change in pressure between two consecutive iterations is below some specified tolerance; for example, $\delta p/p_{max} < 10^{-5}$.

(7) The advanced time quantities become the previous time quantities, and Steps 1 through 6 are repeated for the next time cycle.

The value of $\Delta\tau$ in Equation (87) must be chosen so as to ensure convergence of the iteration scheme. In Appendix A, the pressure field is viewed as the iterative solution of a set of algebraic equations whose convergence properties are examined. To obtain a convergent scheme, the analysis shows that $\Delta\tau$ must be of the form

$$\Delta\tau = \frac{\xi}{\varepsilon_{ijk}\left[\frac{1}{C_I^2}\left(\frac{1}{\Delta t} + \frac{D_{ijk}}{2}\right) + 2\Delta t \sum_{j=1}^{3} \frac{1}{\Delta y_j^2}\right]}, \quad 0 < \xi < 2 \cdot \tag{90}$$

The optimum value of ξ depends on the problem being solved, and ξ may be varied to increase the convergence rate. Although, theoretically, the optimum value of ξ can be determined, to find it by experiment is more feasible. The range $1 \leqslant \xi \leqslant 1.8$ has been observed to usually be appropriate.

2. NUMERICAL BOUNDARY CONDITIONS

Five types of boundary conditions may be applied at the walls of the computing mesh: (1) free-slip, (2) no-slip, (3) inflow, (4) outflow, and (5) pressure. The prescription of these conditions consists of appropriately fixing the velocities, densities, pressures, and specific internal energies in fictitious boundary cells which surround the computing mesh. This process is illustrated in Figure 3. The boundary conditions are set before and after each iteration. The reader should keep in mind that this section only indicates how to treat the various possible boundary conditions numerically and not what constitutes a proper set. A more complete discussion of boundary conditions can be found in References 55 through 57.

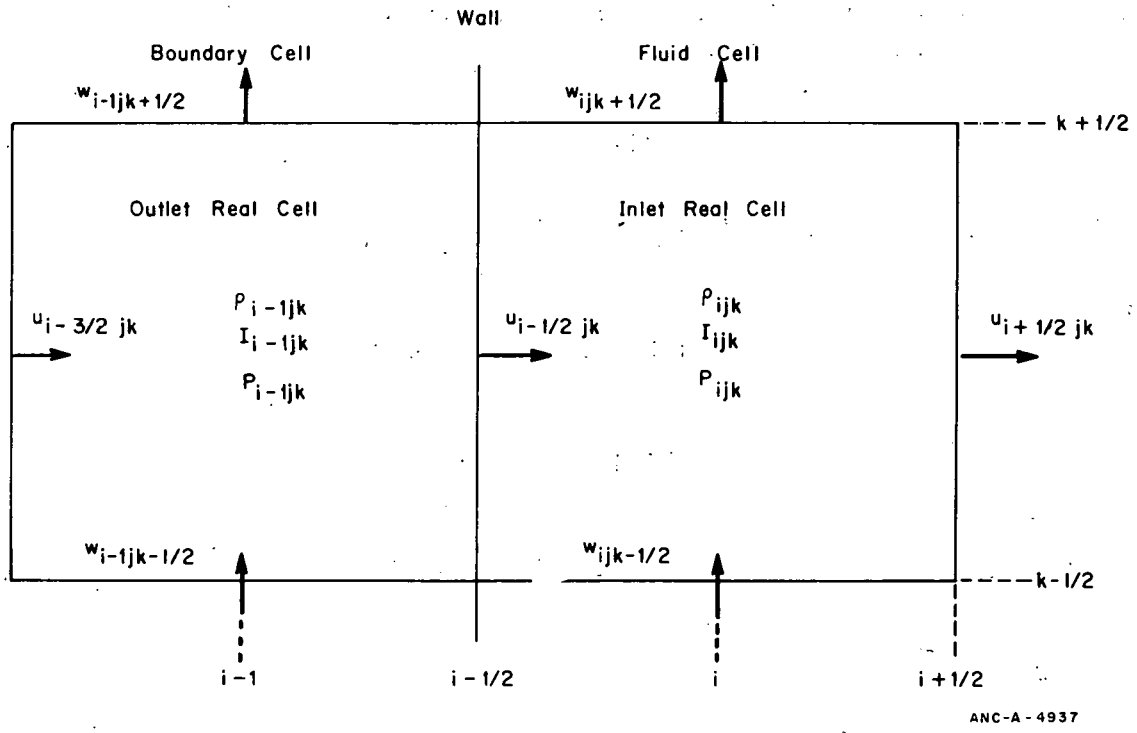

Fig. 3 Position of variables in the (i, k) plane for left wall boundary conditions.

2.1 Free-Slip

A free-slip adiabatic boundary represents a plane of symmetry or a nonadhering surface that exerts no drag on the fluid; that is, $\frac{dv}{dx} = 0$. The normal velocity component, mass flux, and heat flux are zero. The pressure need not be set because the normal velocity is not calculated. The free-slip boundary conditions are

$$u_{i-1/2jk} = 0$$

$$v_{i-1j+1/2k} = v_{ij+1/2k}$$

$$w_{i-1jk+1/2} = w_{ijk+1/2}$$

$$\rho_{i-1jk} = \rho_{ijk}$$

$$I_{i-1jk} = I_{ijk} \quad . \tag{91}$$

2.2 No-Slip

A no-slip adiabatic boundary represents a viscous boundary that exerts a drag on the fluid. This boundary condition is implemented by setting the tangential velocity to zero. The no-slip boundary conditions are

$$u_{i-1/2jk} = 0$$

$$v_{i-jk+1/2k} = -v_{ij+1/2k}$$

$$w_{i-1jk+1/2} = -w_{ijk+1/2}$$

$$\rho_{i-1jk} = \rho_{ijk}$$

$$I_{i-1jk} = I_{ijk} \quad . \tag{92}$$

2.3 Inflow

An inflow boundary allows fluid to enter the system at a prescribed normal velocity, u_R, which may vary with time. The other velocities are either zero or free-slip conditions are used. The specific internal energy I_B is prescribed. The pressure need not be fixed and the density is extrapolated.

The inflow boundary conditions are

$$u_{i-1/2jk} = u_B$$

$$v_{i-1j+1/2k} = \pm v_{ij+1/2k}$$

$$w_{i-1jk+1/2} = \pm w_{ijk+1/2}$$

$$\rho_{i-1jk} = \rho_{ijk}$$

$$I_{i-1jk} = I_B . \tag{93}$$

A properly posed problem would still exist if the roles of ρ and I were to be interchanged; that is, if the inlet density were to be prescribed and the internal energy were to be extrapolated.

2.4 Outflow

A number of different types of outflow boundary conditions can be used. Each type has its own characteristics.

A prescribed outflow boundary allows fluid to be removed from the system at a given rate. This condition is implemented by the following formulas:

$$u_{i-1/2jh} = u_B$$

$$v_{ij+1/2h} = \pm v_{i-1j+1/2k}$$

$$w_{ij+1/2k} = \pm w_{i-1j+1/2k}$$

$$\rho_{ijk} = \rho_{i-1jk}$$

$$I_{ijk} = I_{i-1jk} . \tag{94}$$

A continuative outflow boundary allows fluid to leave the system at a rate determined in such a manner as to have minimal effects on the flow region of interest. Although there is no unique prescription, the idea is to choose conditions which have the least upstream influence. Such a prescription consists of setting the normal velocity on the boundary to that immediately upstream for the explicit stage

$$u_{i-3/2jk} = u_{i-1/2jk} . \tag{95}$$

and letting the normal velocity change freely during the iteration stage. The other variables are set as for the free-slip case.

An extrapolative outflow boundary serves the same purpose as does the continuative one. It differs in that the variables in the fictitious cells are set such that variables in the real cell lying on the boundary are the averages of the values in the adjacent real and fictitious cells; that is:

$$
\begin{aligned}
u_{i+1/2jk} &= 2u_{i-1/2jk} - u_{i-3/2jk} \\
v_{ij+1/2k} &= 2v_{i-1j+1/2k} - v_{i-2j+1/2k} \\
w_{ijk+1/2} &= 2w_{i-1jk+1/2} - w_{i-2jk+1/2} \\
\rho_{ijk} &= 2\rho_{i-1jk} - \rho_{i-2jk} \\
I_{ijk} &= 2I_{i-1jk} - I_{i-2jk} \\
p_{ijk} &= 2p_{i-1jk} - p_{i-2jk} \quad .
\end{aligned}
\tag{96}
$$

2.5 Outlet Pressure

For specified pressure boundary conditions, the pressure in the fictitious boundary cells is set according to

$$p_{ijk} = p_B \quad .$$

The other variables are set as for the continuative or extrapolative case.

3. ACCURACY AND STABILITY

The basic accuracy restriction on the size of the time step is that fluid should not flow across more than one computational cell during each time step; that is:

$$\Delta t < \text{minimum} \left[\frac{\Delta x}{|u|} , \frac{\Delta y}{|v|} , \frac{\Delta z}{|w|} \right] \quad . \tag{97}$$

This is an accuracy condition because the finite difference forms used to represent the convective fluxes assume exchanges only between adjacent cells. However, linearizing the difference equations and performing a Fourier analysis on them reveals that this is also a stability condition[52]. The linear analysis further reveals that for central differencing, the kinematic viscosity must be sufficiently large to insure stability; that is:

$$\frac{\left(\mu+\mu_T\right)}{\tilde{\rho}} > \frac{\Delta t}{2} \quad \text{maximum} \left[u^2, v^2, w^2\right] \quad . \tag{98}$$

In addition, the time step is restricted by the conditions

$$\frac{\left(\mu+\mu_T\right)}{\tilde{\rho}} \Delta t < \frac{1}{2\left(\frac{1}{(\Delta x)^2} + \frac{1}{(\Delta y)^2} + \frac{1}{(\Delta z)^2}\right)} \tag{99}$$

and

$$\frac{k + k_T}{\tilde{\rho}\, C_p} \Delta t < \frac{1}{2\,\frac{1}{(\Delta x)^2} + \frac{1}{(\Delta y)^2} + \frac{1}{(\Delta z)^2}} \tag{100}$$

which limit the distances over which momentum and heat diffuse during one time step to be less than one cell width. Equations (99) and (100) must be observed for both donor cell or centered differencing.

Truncation errors can be obtained by expanding in a Taylor series each term in the finite difference equations about a common point (x, y, z, t) and retaining the lowest order terms which contribute to second spatial derivatives or diffusional terms[58]. A portion of the truncation error in the one-dimensional momentum equation for centered differencing is[59]

$$\left[\left(c_I^2 - 3u^2\right) \frac{\Delta t}{2} - \frac{u(\Delta x)^2}{2} \frac{\partial \rho}{\partial x}\right] \frac{\partial^2 u}{\partial x^2} \quad . \tag{101}$$

The first term is negative if $u^2 > c_I^2/3$ and results in a negative coefficient of the second derivative of u. Donor cell differencing removes this potentially unstable situation.

Since the energy equation, Equation (85), is explicit, donor cell differencing must be used to remove the convective instability that results from centered differencing.

V. EXAMPLE APPLICATIONS

In this section, two applications of the preceding equations and numerical method are given. The code used is called SCORE - EVET. The first application concerns a simple problem that has a known analytic steady state solution. The problem was chosen so that results could be compared with the known solution. The second application was run to demonstrate the capability of the code to handle recirculation and reverse flow situations.

The first application is for plane parallel flow in a straight channel. The friction term F_i in Equation (23) was taken as linear with respect to the velocity; that is:

$$F_i = A\tilde{v}_i \tag{102}$$

The problem was run with no heat sources and no pressure volume work term. The results were compared with an analytic solution for steady state flow[60]. Figure 4 shows the mean velocity profiles as calculated by the code and from the known analytic solution. The agreement is excellent.

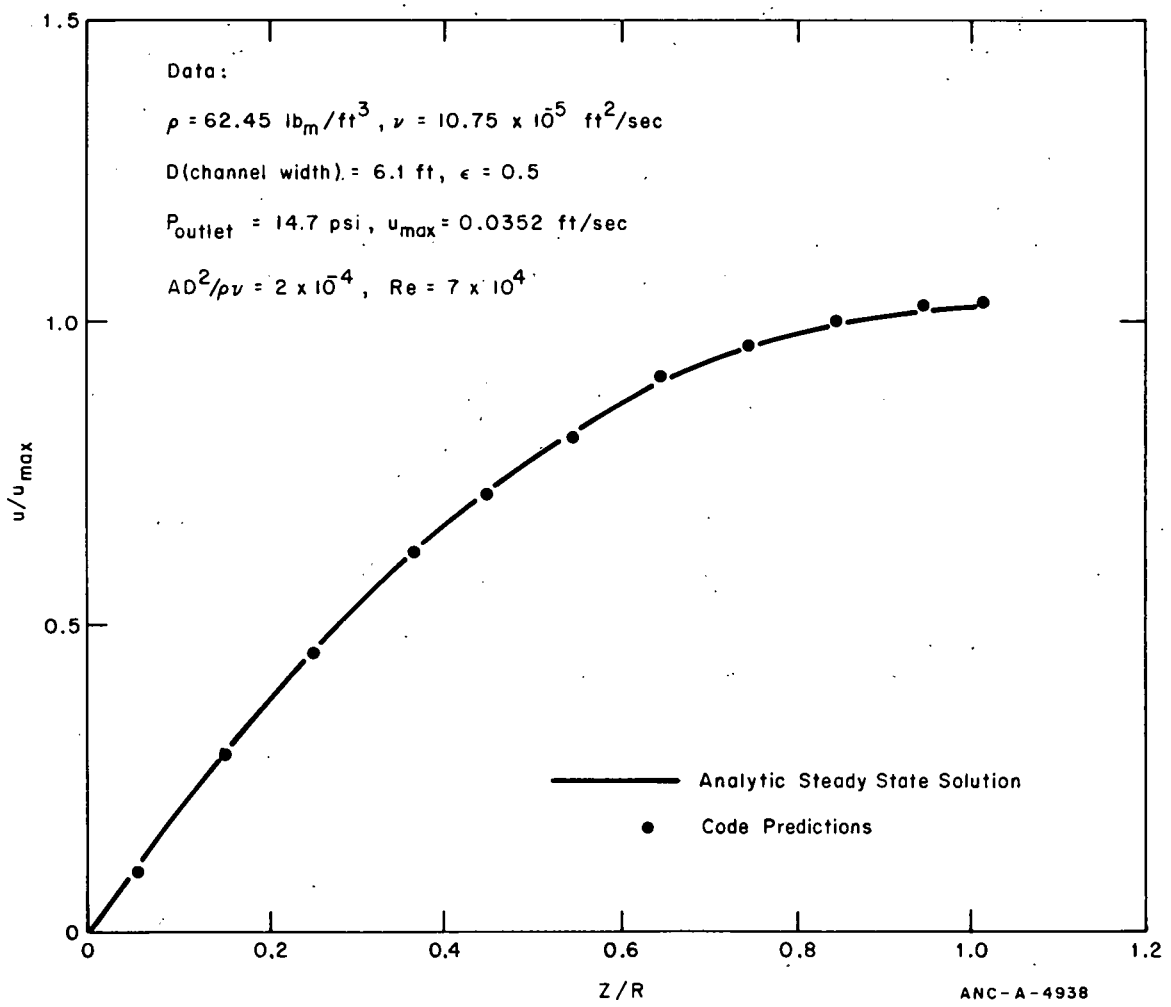

Fig. 4 Porous media channel flow.

The second application is the calculation of the velocity distribution for the flow of liquid water in the rectangular region shown in Figure 5. As indicated in Figure 5, the region is composed of one smaller portion with $\epsilon = 0.25$ and one large portion with $\epsilon = 0.50$. Liquid water is introduced at a constant, uniform velocity over one half of the bottom of the region. The remaining one half of the inlet represents a blockage to the flow. The axial friction force was evaluated using the Colebrook formula [Equation (14)], and the transverse friction force was calculated using a correlation for laminar flow developed for tube bundles[23, 24]. The wall heat supply per unit volume, Q_w, was taken to be zero.

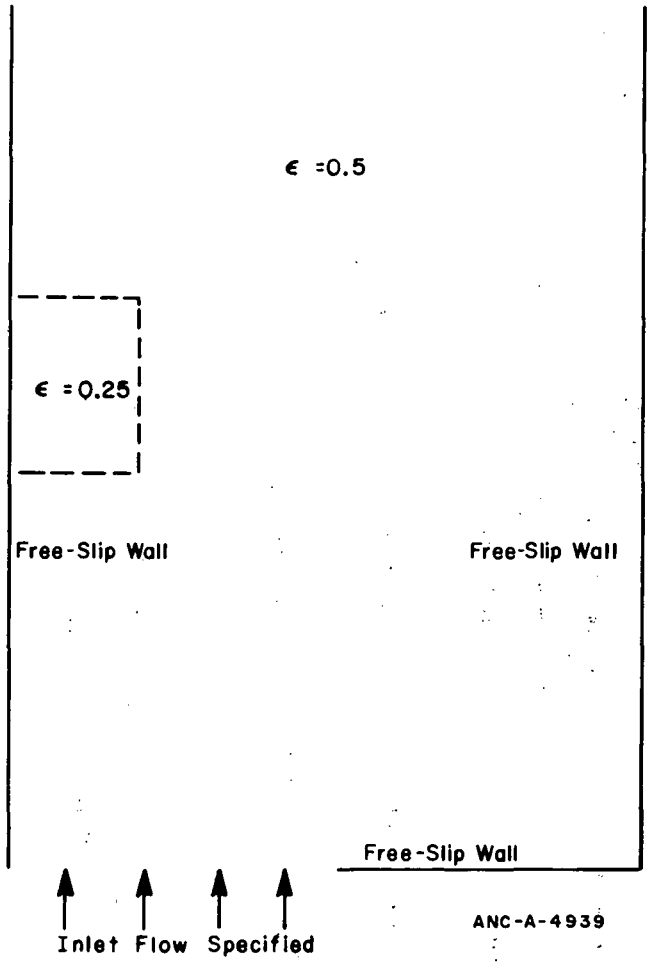

Fig. 5 Calculation region and boundary conditions for blockage problem.

The results of the calculation are shown in Figure 6. The velocity vectors show the fluid turning at the $\epsilon = 0.25$ portion and a recirculating flow behind the inlet blockage. These results show the capability of the codes to carry out calculations involving flow reversal recirculation.

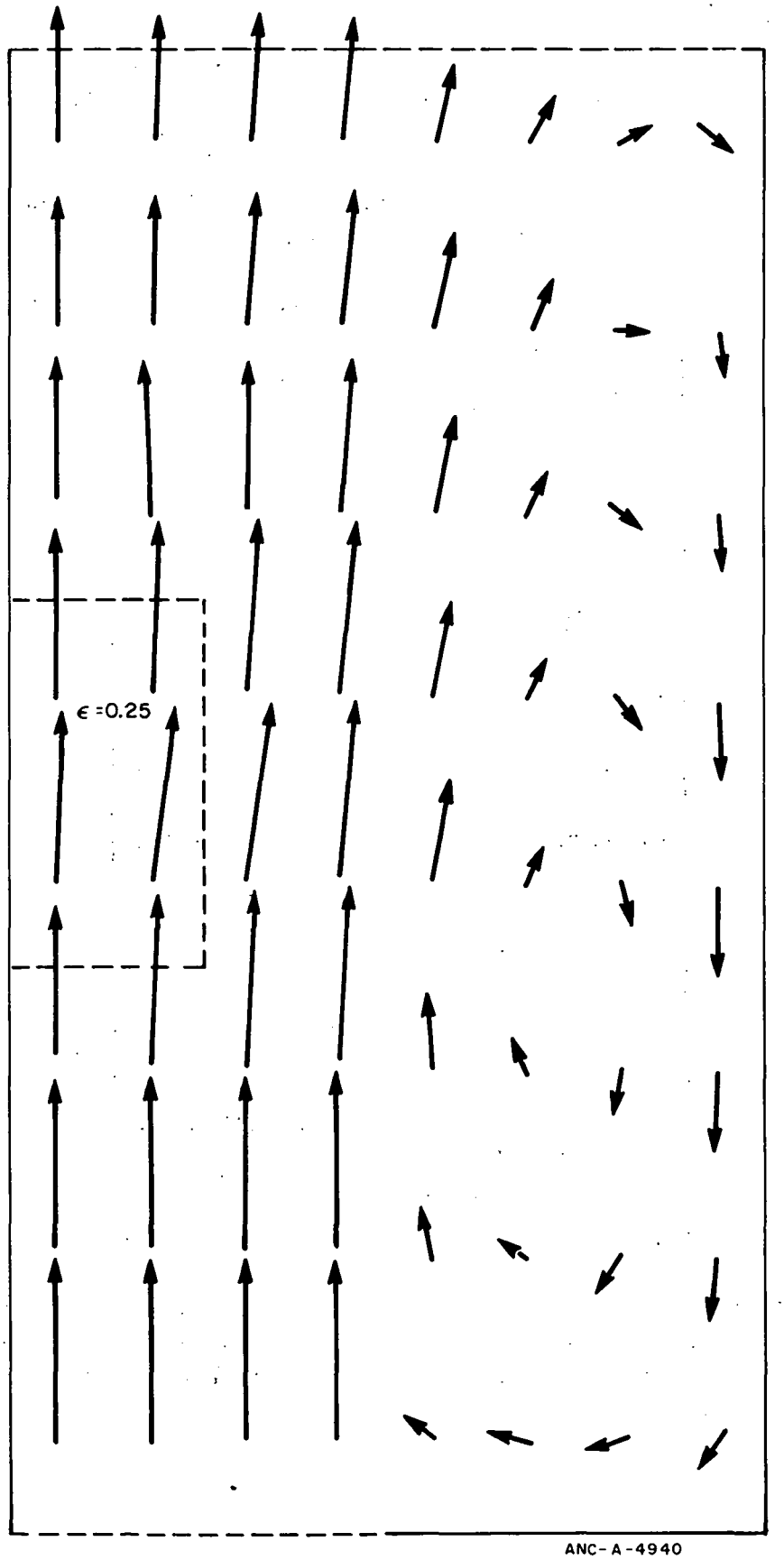

Fig. 6 Steady state velocity vectors for blockage problem.

VI. CONCLUSIONS

The present model includes the full Navier-Stokes equations and thus can calculate natural circulation flows or flows with large transverse velocity components. The numerical solution scheme solves the equations as an initial value problem in time and boundary value problem in space. Consequently, flow reversals and recirculation are easily handled and downstream flow effects are accounted for correctly.

The model is applicable to calculations of flows in a wide variety of engineering equipment as well as flows in porous media.

VII. REFERENCES

1. B. E. Launder and D B. Spalding, *Mathematical Models of Turbulence*, New York: Academic Press, 1972.

2. D. S. Rowe and C. W. Angle, *Crossflow Mixing Between Parallel Flow Channels During Boiling, Part 1: COBRA - Computer Program for Coolant Boiling in Rod Arrays*, BNWL-371-1 (1967).

3. D. S. Rowe, *COBRA-II: A Digital Computer Program for Thermal-Hydraulic Subchannel Analysis of Rod Bundle Nuclear Fuel Elements*, BNWL-1229 (1970).

4. D. S. Rowe, *COBRA-III: A Digital Computer Program for Steady-State and Transient Thermal-Hydraulic Analysis of Rod Bundle Nuclear Fuel Elements*, BNWL-B-82 (1971).

5. D. S. Rowe, *An Improved Mathematical Model for Transient Subchannel Analysis of Rod Bundle Nuclear Fuel Elements*, ASME Preprint 72-WA/H7-49 (1972).

6. R. W. Bowring, *HAMBO, A Computer Programme for the Subchannel Analysis of the Hydraulic and Burnout Characteristics of Rod Clusters, Part 1 General Description*, AEEW-R524 (1967).

7. R. W. Bowring, *HAMBO, A Computer Programme for the Subchannel Analysis of the Hydraulic and Burnout Characteristics of Rod Clusters, Part 2 The Equations*, AEEW-R582 (1968).

8. E. di Capua and R. Riccardi, *Forced Convection Burnout and Hydrodynamic Instability Experiments for Water at High Pressure, Part VIII Analysis of Burnout Experiments on 3x3 Rod Bundles with Uniform and Non-Uniform Heat Generation*, EUR-4875e (1972).

9. V. Marinelli, L. Pastori, B. Kjellen, "Experimental Investigation of Mass Velocity Distribution and Velocity Profiles in an LWR Rod Bundle", *European Two-Phase Flow Group Meeting, Rome, Italy, 1972*.

10. Babcock & Wilcox Company, *TEMP, Thermal Enthalpy Mixing Program*, BAW-10021 (1970).

11. S. G. Beus, J. H. Anderson, R. J. De Cristofaro, *HOTROD: A Computer Program for Subchannel Analysis of Coolant Flow in Rod Bundles*, WAPD-TM-1070 (1973).

12. R. W. Bowring, "Heat Transfer and Fluid Flow in Complex Geometries - Assumptions and Deduction of Main Subchannel Codes" *European Two-Phase Flow Group Meeting, Rome, Italy, 1972*.

13. F. P. Berger, "International Meeting on Reactor Heat Transfer at Karlsruke (A Critical Review)", *Annals of Nuclear Science and Engineering, 1* (1974) pp 157-161.

14. J. C. Slattery, *Momentum, Energy and Mass Transfer in Continua*, New York: McGraw-Hill Book Company, Inc. 1972.

15. K. Maubach and K. Rehme, "Pressure Drop for Parallel Flow Through a Roughened Rod Cluster", *Nuc. Eng. Design, 25*, (1973) pp 369-378.

16. C. Savatteri, *Friction Factors of a Cluster of 19 Rods*, KFK 1588 (EUR 4728) (1972).

17. K. Rehme, "Pressure Drop Performance of Rod Bundles in Hexagonal Arrangements", *Int. J. Heat Mass Transfer, 15* (1972) pp 2,499-2,517.

18. K. Rehme, "Simple Method of Predicting Friction Factors of Turbulent Flow in Non-Circular Channels", *Int. J. Heat Mass Transfer, 16* (1973) pp 933-950.

19. W. Eifler and R. Nijsing, "Experimental Investigation of Velocity Distribution and Flow Resistance in a Triangular Array of Parallel Rods", *Nuc. Eng. Design, 5* (1967) pp 22-42.

20. R. Nijsing and W. Eifler, "Analysis of Liquid Metal Heat Transfer in Assemblies of Closely Spaced Fuel Rods", *Nuc. Eng. Design, 10* (1969) pp 21-54.

21. O. E. Dwyer and H. C. Berry, "Heat Transfer to Liquid Metals Flowing Turbulently and Longitudinally through Closely Spaced Rod Bundles", *Nuc. Eng. Design, 23* (1972) pp 295-308.

22. J. Malak, J. Heina, J. Schmid, "Pressure Losses and Heat Transfer in Non-Circular Channels with Hydraulically Smooth Walls", *Int. J. Heat Mass Trans., 18* (1975) pp 139-149.

23. K. J. Bell, *Final Report of the Cooperative Research Program on Shell and Tube Heat Exchangers*, University of Delaware Engineering Experiment Station Bulletin No. 5 (1963).

24. O. P. Bergelin, G. A. Brown, S. C. Doberstein, "Heat Transfer and Fluid Friction During Flow Across Banks of Tubes -IV: A Study of the Transition Zone Between Viscous and Turbulent Flow", *Trans. ASME, 74* (1952) pp 953-960.

25. S. C. Ko and W. H. Graf, "Drag Coefficient of Cylinders in Turbulent Flow", *Proc. ASCE, 98* No. Hy5 (1972) pp 897-912.

26. I. C. Finlay and T. McMillian, "Pressure Loss During Air/Water Mist Flow Across a Staggered Bank of Tubes", *Int. J. Multi-Phase Flow, 1* (1974) pp 604-606.

27. S. Ishigai, E. Nishikowa, K. Nishimura, K. Cho, "Experimental Study on Structure of Gas Flow in Tube Banks with Tube Axes Normal to Flow", *Bulletin JSME, 15* (1972) pp 949-956.

28. J. R. S. Thom, "Prediction of Pressure Drop During Forced Circulation Boiling of Water", *Int. J. Heat Mass Transfer,* 7 (1964) pp 709-724.

29. D. R. H. Beattie, "A Note on the Calculation of Two-Phase Pressure Losses", *Nuc. Engineering Design, 25* (1973) pp 395-402.

30. D. R. H. Beattie, *Two-Phase Pressure Losses Flow Regime Effects and Associated Phenomena*, AAEC TM 589 (1971).

31. D. Chisholm, "A Theoretical Basis for the Lockhart - Martinelli Correlation for Two-Phase Flow", *Int. J. Heat Mass Transfer, 10* (1967) pp 1,767-1,778.

32. D. Chisholm, "The Influence of Mass Velocity on Friction Pressure Gradients During Steam-Water Flow", *Proc. Instn. Mech. Engrs., 182*, Pt 3H (1968) pp 336-341.

33. J. G. Collier, "Two-Phase Gas-Liquid Pressure Drop and Void Fraction - A Review of the Current Position", 1974 European Two-Phase Flow Conference, Harwell, 1974.

34. C. Lombardi and E. Pedrocchi, "A Pressure Drop Correlation in Two-Phase Flow", *Energia Nucleare, 19* (1972) pp 91-99.

35. R. W. Lockhart and R. C. Martinelli, "Proposed Correlation of Data for Isothermal Two-Phase, Two-Component Flow in Pipes", *Chem. Engng. Progr., 45* (1949) pp 39-48.

36. C. J. Baroczy, *Correlation of Liquid Fraction in Two-Phase Flow with Application to Liquid Metals*, NAA-SR-8171 (1963).

37. J. M. Turner and G. B. Wallis, *The Separate - Cylinders Model of Two-Phase Flow*, Dartmouth College Report NYO-3114-6 (1965).

38. D. Butterworth, *A Comparison of Some Void - Fraction Relationships*, AERE-M2619 (1974).

39. S. L. Smith, "Void Fractions in Two-Phase Flow, A Correlation Based Upon an Equal Velocity Head Model", *Proc. Instn. Mech. Engrs., 184*, Pt 1 (1970) pp 647-664.

40. S. G. Bankoff, "A Variable Density Single-Fluid Model for Two-Phase Flow with Particular Reference to Steam-Water Flow", *Trans. ASME J. Heat Trans., 82* (1960) pp 265-272.

41. S. Y. Ahmad, "Axial Distribution of Bulk Temperature and Void Fraction in a Heated Channel with Inlet Subcooling", *Trans. ASME J. Heat Trans., 92* (1970) pp 595-609.

42. D. S. Rowe, *Measurement of Turbulent Velocity, Intensity, and Scale in Rod Bundle Flow Channels* BNWL-1736 (1973).

43. D. S. Rowe and C. C. Chapman, *Measurement of Turbulent Velocity, Intensity, and Scale in Rod Bundle Flow Channels Containing a Grid Spacer*, BNWL-1757 (1973).

44. J. T. Rogers and R. G. Rosehart, *Mixing by Turbulent Interchange in Fuel Bundles, Correlations and Inferences*, ASME paper No. 72-HT-53 (1972).

45. K. P. Galbraith and J. G. Knudsen, *Turbulent Mixing Between Adjacent Channels for Single Phase Flow in a Rod Bundle*, AICHE Preprint 19 (1971).

46. B. Kjellstrom, *Pressure Drop, Velocity Distributions and Turbulence Distributions for Flow in Rod Bundles*, AE-RL-1236 (1970).

47. B. Kjellstrom, *Transport Processes in Turbulent Channel Flow*, AE-RL-1344 (1972).

48. D. R. H. Beattie, "Two-Phase Flow Structure and Mixing Length Theory", *Nuc. Eng. Design, 21* (1972) pp 46-64.

49. K. V. Moore and W. H. Rettig, *RELAP4 - A Computer Program for Transient Thermal-Hydraulic Analysis*, ANCR-1127 (1973).

50. J. G. Collier, *Convective Boiling and Condensation*, New York: McGraw-Hill Book Co., Inc., 1972.

51. W. M. Rohsenow, "Status of and Problems in Boiling and Condensation Heat Transfer", *Progress in Heat and Mass Transfer, Vol. 6*, New York: Pergamon Press, 1972.

52. C. W. Hirt, and J. L. Cook, "Calculating Three-Dimensional Flows Around Structures and Over Rough Terrain", *J. Comp. Phys., 8* (1972) pp 197-340.

53. F. H. Harlow, and A. A. Amsden, "A Numerical Fluid Dynamics Calculation Method for All Flow Speeds", *J. Comp. Phys., 8* (1971) pp 197-213.

54. J. A. Viecelli, "A Computing Method for Incompressible Flows Bounded by Moving Walls", *J. Comp. Phys., 8* (1971) pp 119-143.

55. C. K. Chu and A. Sereny, "Boundary Conditions in Finite Difference Fluid Dynamic Codes", *J. Comp. Phys., 15* (1974) pp 476-491.

56. G. Moretti, "Importance of Boundary Conditions in the Numerical Treatment of Hyperbolic Equations", *Phys. Fluids Supplement II, 12* (1969) pp 13-19.

57. J. H. Chen, "Numerical Boundary Conditions and Computational Modes", *J. Comp. Phys., 13* (1973) pp 522-535.

58. C. W. Hirt, "Heuristic Stability Theory for Finite-Difference Equations", *J. Comp. Phys., 2* (1968) pp 339-355.

59. F. H. Harlow, and A. A. Amsden, "Numerical Calculation of Almost Incompressible Flow", *J. Comp. Phys., 3* (1968) pp 80-93.

60. J. C. Slattery, "Single-Phase Flow Through Porous Media", *AICHE Journal, 15*, No. 6 (1969) pp 866-872.

APPENDIX A

LINEAR STABILITY ANALYSIS

THIS PAGE

WAS INTENTIONALLY

LEFT BLANK

APPENDIX A

LINEAR STABILITY ANALYSIS

The following iteration scheme for the solution of the mass conservation and linear momentum equations in one-dimensional conservative form is considered:

$$(\varepsilon\rho v)^{m+1}_{\ell+1/2} = (\varepsilon\rho v)^{n}_{\ell+1/2} - \Delta t\, \varepsilon^{n}_{\ell+1/2} \frac{(P^{m}_{\ell+1} - P^{m}_{\ell})}{\Delta X} + R^{n}_{\ell+1/2} \tag{A-1}$$

$$S^{m}_{\ell} = \frac{(\varepsilon\rho)^{m}_{\ell} - (\varepsilon\rho)^{n}_{\ell}}{\Delta t} + \frac{(\varepsilon\rho v)^{m+1}_{\ell+1/2} - (\varepsilon\rho v)^{m+1}_{\ell-1/2}}{\Delta X} \tag{A-2}$$

$$p^{m+1}_{\ell} = p^{m}_{\ell} - \Delta\tau S^{m} \tag{A-3}$$

$$\rho^{m+1}_{\ell} = f(p^{m+1}_{\ell},\ I^{n+1}_{\ell}) \tag{A-4}$$

where

m = iteration number

n = old time level

R^{n}_{k} = explicit calculation of convection, viscous, friction, and body force terms.

In Equations (A-1) through (A-4), a one-dimensional form has been assumed for convenience. Linearizing the state equation over a time step and substituting Equations (A-4) and (A-1) into Equation (A-2) and then using the result in Equation (A-3) gives

$$p^{m+1}_{\ell} = p^{m}_{\ell} - \Delta\tau \left[\frac{\varepsilon^{n}_{\ell}}{C_I^2} \frac{(p^{m}_{\ell} - p^{n}_{\ell})}{\Delta t} - \frac{\Delta t}{(\Delta X)^2} \varepsilon^{n}_{\ell} (p^{m}_{\ell+1} - 2p^{m}_{\ell} + p^{m}_{\ell-1}) \right.$$

$$\left. + (\varepsilon\rho v)^{n}_{\ell+1/2} - (\varepsilon\rho v)^{n}_{\ell-1/2} + R^{n}_{\ell+1/2} - R^{n}_{\ell-1/2} \right] . \tag{A-5}$$

In obtaining Equation (A-5), ϵ has been assumed slowly varying in time and space, and its time and space derivatives were neglected.

When the iteration has converged, an equation similar to Equation (A-5) results except that all the m and m+1 superscripts have become n+1. Subtraction of this converged pressure equation from Equation (A-5) gives

$$\delta p_{\ell}^{m+1} = \delta p_{\ell}^{m} - \Delta t \left[\frac{\epsilon_{\ell}^{n}}{c_t^2} \frac{\delta p^{m}}{\Delta t} - \frac{\Delta t}{(\Delta x)^2} \epsilon_{\ell}^{n} \left(\delta p_{\ell+1}^{m} - 2\delta p_{\ell}^{m} + \delta p_{\ell-1}^{m} \right) \right] \tag{A-6}$$

where

$$\delta p_{\ell}^{m+1} = p_{\ell}^{m+1} - p_{\ell}^{n+1}$$

is the deviation of the pressures from p_{ℓ}^{n+1}.

The iteration scheme is convergent if $\delta p_{\ell}^{m} \to 0$ as $m \to \infty$. If a perturbation of the form

$$\delta p_{\ell}^{m} = A\xi^{m} e^{i\alpha \ell \Delta x} \tag{A-7}$$

is substituted into Equation (A-6), it is seen that the amplification factor ξ must satisfy

$$\xi = 1 - \Delta\tau \left[\frac{\epsilon_{\ell}^{n}}{c_I^2 \Delta t} - \frac{\Delta t}{(\Delta x)^2} \epsilon_{\ell}^{n} \left(2\cos(\alpha \Delta x) - 2 \right) \right] . \tag{A-8}$$

Now if $\delta p_{\ell}^{m} \to 0$ as $m \to \infty$ for all wave numbers α, a necessary condition for convergence is

$$|\xi| < 1 \text{ for all } \alpha. \tag{A-9}$$

In general, $\xi < 1$ and the least favorable case (as α varies) occurs as ξ approaches -1. ξ is most negative when $\cos(\alpha \Delta x)$ equals -1 and to have $\xi > -1$ in this case requires

$$-1 < 1 - \Delta\tau \epsilon_{\ell}^{n} \left(\frac{1}{c_I^2 \Delta t} + \frac{4\Delta t}{(\Delta X)^2} \right)$$

or

$$\Delta\tau < \frac{2}{\epsilon_{\ell}^{n} \left(\frac{1}{c_I^2 \Delta t} + \frac{4\Delta t}{(\Delta X)^2} \right)} . \tag{A-10}$$

If the analysis had been carried out in three dimensions and in nonconservative form, Equation (A-10) would be replaced by

$$\Delta\tau < \frac{2}{\varepsilon^n_{ijk}\left[\frac{1}{C_I^2}\left(\frac{1}{\Delta t} + (\nabla\cdot\underset{\sim}{u})_{ijk}\right) + 4\Delta t \sum_{i=1}^{3}\frac{1}{(\Delta X_i)^2}\right]} \qquad \text{(A-11)}$$

A similar analysis shows that if the new iterates for pressure are used as soon as they become available, $\Delta\tau$ is limited by

$$\Delta\tau < \frac{2}{\varepsilon^n_{ijk}\left[\frac{1}{C_I^2}\left(\frac{1}{\Delta t} + (\nabla\cdot\underset{\sim}{u})_{ijk}\right) + 2\Delta t \sum_{i=1}^{3}\frac{1}{(\Delta X_i)^2}\right]} \qquad \text{(A-12)}$$

for convergence of the iteration scheme.

DISTRIBUTION RECORD FOR ANCR-1207

External

296 - NRC-4, Water Reactor Safety Research Analysis Development

2 - H. J. C. Kouts, NRC

Internal

1 - Chicago Patent Group - ERDA
9800 South Cass Avenue
Argonne, Illinois 60439

3 - A. T. Morphew, Classification and Technical Information Officer
ERDA-ID
Idaho Falls, Idaho 83401

1 - R. J. Beers, ID

1 - P. E. Litteneker, ID

1 - R. E. Swanson, ID

1 - V. A. Walker, ID

1 - R. E. Wood, ID

34 - Special Internal Distribution

11 - INEL Technical Library

46 - Author

Total Copies Printed - 398